CT-697-58Z
Don.-2012

xx(199748.1)

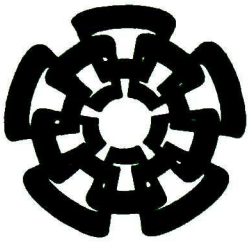

Centro de Investigación y de Estudios Avanzados
del Instituto Politécnico Nacional
Unidad Guadalajara

Diseño e implementación de la técnica de calibración LRRM

Tesis que presenta:
Diego Orozco Navarro

para obtener el grado de:
Maestro en Ciencias

en la especialidad de:
Ingeniería Eléctrica

Directores de tesis:
Dr. José Raul Loo Yau
Dr. J. Apolinar Reynoso Hernández

CINVESTAV del IPN Unidad Guadalajara, Guadalajara, Jalisco, Febrero de 2012.

ID. 199731-2001

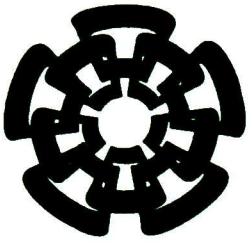

Centro de Investigación y de Estudios Avanzados
del Instituto Politécnico Nacional
Unidad Guadalajara

Design and implementation of LRRM calibration technique

A thesis presented by:
Diego Orozco Navarro

to obtain the degree of:
Master of Science

in the subject of:
Electrical Engineering

Thesis Advisors:
Dr. José Raul Loo Yau
Dr. J Apolinar Reynoso Hernández

CINVESTAV del IPN Unidad Guadalajara, Guadalajara, Jalisco, February 2012.

Diseño e implementación de la técnica de calibración LRRM

Tesis de Maestría en Ciencias
Ingeniería Eléctrica

Por:
Diego Orozco Navarro
Ingeniería en Electrónica y Comunicaciones
Instituto Tecnológico de Estudios Superiores de Monterrey Campus Guadalajara 2002-2007

Becario de CONACYT, expediente no. 40456

Directores de tesis:
Dr. José Raul Loo Yau
Dr. J Apolinar Reynoso Hernández

CINVESTAV del IPN Unidad Guadalajara, Febrero de 2012.

Design and implementation of LRRM calibration technique

Master of Science Thesis
In Electrical Engineering

By:
Diego Orozco Navarro
Engineer in Electronics and Communication
Instituto Tecnológico de Estudios Superiores de Monterrey Campus Guadalajara 2002-2007

Scholarship granted by CONACYT, No. 40456

Thesis Advisors:
Dr. José Raul Loo Yau
Dr. J Apolinar Reynoso Hernández

CINVESTAV del IPN Unidad Guadalajara, February, 2012.

This page was left intentionally blank

Contents

Content of Figures

Resumen

El analizador de redes vectorial (ARV) es un equipo de medición que se utiliza para caracterizar y verificar dispositivos y/o sistemas a muy altas frecuencias. Un ARV mide en principio los parámetros S, que no son más que relaciones de ondas incidentes y reflejadas de cada puerto del dispositivo bajo prueba (DBP). Las ondas incidentes y reflejadas son dependientes de lo que se encuentre entre el DBP y el ARV. Por lo tanto, es necesario realizar un proceso de calibración con el fin de establecer el plano de referencia justo en el DBP. Así, todo lo que se encuentre fuera del plano de referencia, se considera como errores, su corrección y la medición será con referencia al DBP.

Los errores se pueden eliminar a través de un proceso de calibración. Este proceso es en realidad un desarrollo matemático basado en teoría de flujo y de álgebra lineal, en el cual los errores son cajas que se representan con un modelo de 8 o 12 términos de error. Por un lado, el modelo de 8 términos ha demostrado ser suficiente para calibrar un ARV. Por otro lado, para eliminar los errores de la medición, se requieren de estándares como por ejemplo elementos reflectores (corto circuitos y/o circuitos de alta impedancia) o líneas de transmisión no reflectoras.

Existen diferentes técnicas de calibración como la TRL, TAR, TRM, TRRM, etc. Las técnicas de calibración reciben su nombre en función de los estándares que se utilizan. En ese mismo orden de idea, en este trabajo se desarrolló una base de pruebas universal para poder realizar mediciones de los parámetros S de los estándares de calibración así como de transistores de Nitruro de Galio (GaN). Además se presenta un algoritmo diferente al convencional para la técnica de calibración TRRM.

El nuevo algoritmo se validó comparándolo con la técnica TRL, que es una técnica ampliamente utilizada y conocida. Los parámetros S del transistor, empleando el nuevo algoritmo de la TRRM son muy similares con los datos obtenidos con la TRL. Las diferencias obtenidas entre la TRRM y TRL son atribuidas a problemas de contacto debido a la mecánica de la base de pruebas, permitiendo solo medir hasta 6 GHz.

Abstract

The Vector Network Analyzer (VNA) is a measurement device utilized for high frequency devices and systems characterization. The VNA measures the S parameters, which are ratios of the reflected wave to the incident wave at each port of the Device Under Test (DUT). These incident and reflected waves depend on the position where they are measured (reference plane). For this, a calibration process is necessary to help in establishing the reference plane at the DUT, everything else beyond the reference plane will be considered as errors.

The errors can be removed by means of a calibration process. This process is a mathematical development based on flow graph theory and linear algebra, in which the errors are taken as "error boxes". In practice, two models are the most utilized: the eight term error model and the twelve term error model. In order to eliminate the measurement errors, standards are needed, e.g.: Reflects (Open and Short), Loads and non-reflective transmission lines. However, the eight term error model has shown to be sufficient for VNA calibration.

Several calibration techniques exist, such as, TRL, TAR, TRM, TRRM, etc. The calibration techniques are named by the standards utilized in their process. Because of the dependency on technology applied to the calibration, in this work a test fixture was designed and fabricated in order to perform S parameters measurements for Galium Nitride (GaN) transistors. In addition, an alternate algorithm to the conventional one is presented for the TRRM calibration technique.

This new algorithm was validated by performing a comparison against the well-known and used TRL calibration technique. It is shown that, the S parameters of the transistor are very close to those from the TRRM and TRL calibration techniques. The subtle differences are attributed to a contact problem in the transition from coaxial to microstrip technology due to mechanical problems presented in the test fixture, where frequencies of up to 6 GHz were reached.

Aknowledgements

The author have been supported by friends, professors, colleagues and institutions throughout the preparation of "Design and Implementation of LRRM calibration technique".

I thank Consejo Nacional de Ciencia y Tecnología (CONACYT) for all the support and scholarship given during my master program, The Centro de Investigación y de Estudios Avanzados (CINVESTAV) del Instituto Politécnico Nacional and the Centro de Investigación Científica y de Educación Superior de Ensenada (CICESE) Baja California provided resources, equipment and support to complete the work.

Ph.D. Raúl Loo Yau, thanks for being not just a teacher, but a counselor who head me through what it was not the best for you but for both, the freedom I had to express my concerns, my complains, my thoughts. Also for doubting and trust me when there were a lot of troubles when demonstrating and implementing the theory of this work.

Ph.D. J Apolinar Reynoso Hernández, I thank you for all the resources, the expertise and provided to get the work done and with your advices improve what have already been done so that I could have a better conclusion of my work.

Father, I thank all your patience, your support. I admire your hard working, your wisdom, your will to never stop learning and all advices that sometimes I did not want to hear but in the end most of them turned out to be true.

Mother, your support, your confidence, you always wanted to know everything about how I was doing. My brothers: Edgar and Fabian who were always showing me different things apart from my master.

Laura, all your patience, your advices, your determination to obtain what you want are some of the things that I have tried to follow from you. Thanks for all your time listening to me in hard moments, supporting me all the time and all what we have shared.

Friends, thanks for the company and all the experiences that we lived through. All the fun and all the friendship has never been gone and even though I lost contact, I have always counted on you.

Finally, I thank the reviewers for getting this work done. With all the corrections, the quality of this work will be shown hopefully and cited by others.

Preface

As technology advances, it requires a high level of component integration, and demands ever lower costs and smaller dimensions. Most RF circuits nowadays are constructed on PCBs (coplanar, microstrip, stripline), whereas, measurement equipment (i.e.: Vector Network Analyzer, Spectrum Analyzer) is constructed over coaxial technology. In addition there exist several side devices constructed with no coaxial technology. For those devices not using coaxial technology, a transition must be made in order to convert from the coaxial coming from the measurement device to the non-coaxial technology used by the device. In addition the transition has to be as efficient as possible to reduce losses and to warrant a maximum energy transfer to the device.

Device characterization plays an important role when measuring, as it yields useful information on how the device behaves at certain ranges. When characterizing a device, can be either to validate a design or know how the device works. Different equipment is used to measure and model components; among them is the Vector Network Analyzer (VNA). When a design is implemented, a VNA measurement will show the differences between the design and how the device is actually functioning, so that, in case a big difference is found, design parameters can be adjusted. For device verification, a vendor may provide data, but the device behavior will not be exactly the same as the data provided, due to the inaccuracies in the manufacturing process and changes in the environment.

A Vector Network Analyzer accurately characterizes the electrical performance of components and circuits, used in more complex systems, by measuring their effect on the amplitude and phase of swept-frequency and swept-power test signals.

The VNA uses coaxial technology, however, for measuring surface mount components placed in either microstrip or coplanar technology, a proper transition must be made with a reference plane displacement, such that the VNA can communicate with the component. The surface mount component is placed on a mechanical device called "test fixture". Wafer devices are connected to a mechanical device called "probe station" which consists of the proper cable transition from coaxial to probes and then to the proper technology used in the wafer.

VNA measurements are always accompanied by errors. Intrinsic errors are characteristic of the physics of the measurement device, its internal components, connections and the fabrication process. Engineers model such systematic errors in order to eliminate them from the measurement. This process, called "calibration", results in a more consistent and accurate reading.

The calibration theory for VNA has yielded different error models for one-port, and two port measurements. Currently, the twelve error term model and the eight error term model are the most used for two port VNA calibration. The twelve error term model is a more accurate model than the eight error term model, but the latter has proved to be sufficient to characterize errors by using flow graph theory and so will be explained in this work.

As with any electronic device, the VNA has to be calibrated through an error term model in order to have reliable measurements and repeatability for consistency. Research is currently being conducted to compute the error terms; it is here where the calibration techniques appear. Several accurate calibration techniques exist, with each technique having advantages and disadvantages. Selecting an appropriate calibration technique for a given process depends on the calibration complexity, accuracy and the frequency range on which the device will be measured.

Device Under Test (DUT) mounted on the test fixture, consists of coaxial interfaces and non-coaxial transmission lines (typically microstrip lines). The test fixture must be designed in order to comply with the DUT in dimensions and work at the desired frequency range. All of these components must be totally or partially known depending on the calibration technique used, so that the de-embedding can be possible and reliable.

In order to have an accurate and pure DUT measurement, the effect of the transitions and transmission lines added to the DUT must be removed from the measurement. The intrinsic errors of the VNA, transitions and part of the

transmission lines that contains the DUT must be removed from the measurement of the DUT. The process of removing these errors is called "de-embedding", where the reference plane is set to the middle of the referene (Thru) line.

There exist several calibration techniques but the most common is the SOLT technique (Short, Open, Load, Thru) (Hewlett-Packard, 1986) which is most often integrated into VNA hardware. As the name implies it uses a thru transmission line, two high reflection coefficient patterns (Short, Open), and an extremely low reflection coefficient pattern (with 50Ω impedance load.

Motivation

High frequency (RF and microwave) circuits and components must be carefully validated before being implemented, because manufacturing and materials are expensive. Computer Aided Design (CAD) software helps in the analysis and gives a good approach to a desired design. However, because the complexity of the analysis grows exponentially, it is time consuming and not all variables can be taken into account. Normally an electromagnetic simulation is made to verify a design, later a physical measurement is taken to obtain a model of the actual design. The design is then improved by making the necessary changes based on the obtained model.

Characterizing devices that work in the RF and the microwave frequency domains implies the use of the VNA. This device can evaluate all type of circuits e.g. filters, amplifiers, transistors, complex multifunction subsystems. The VNA is used because it characterizes any electronic device as a black box with S parameters.

The reason for characterizing devices using S parameters is that such parameters are relatively easy to derive at high frequencies and are directly related to the measurement parameters of interest such as gain, return loss (RL), and reflection coefficient (Γ).

S parameters are extensively used at microwave frequencies as they provide the behavior of the Device Under Test (DUT) with a simple inspection. Moreover, S parameters is a powerful tool that helps in the development of an electrical equivalent circuit model of any device. The accuracy of the model depends directly on how accurate the VNA can measure the S parameters. Hence, the VNA has to be calibrated correctly, this means, eliminate the internal errors, with this purpose, calibration techniques such as, TRL, TRRM, TAR, etc. have been developed.

In the case of in-fixture device characterization, contrary to the coaxial device case, S parameters cannot be measured directly, because the DUT has to be

mounted on a test fixture. This fact implies knowing the losses and establishing a new reference plane in order to obtain the actual S parameters of a DUT. Commercial test fixtures are very expensive, in addition, depending on the calibration technique, the calibration algorithm and the needed calibration standards (Line, Open, Short, Match, etc.) have to be acquired.

There exist different calibration techniques that correct the systematic errors, these techniques receive their names according with the standards used:

- Short-Open-Load-Thru(SOLT)
- Thru-Reflect-Line (TRL)
- Thru-Reflect-Match (TRM)
- Thru-Reflect-Reflect-Match(TRRM)

In order to choose the calibration technique that best fits our needs it will be necessary to focus on which technology is being used, the ease of fabrication, the cost and the frequency range. It should be noted that all factors are important, as the accuracy of the measurements and the application constraints depend on all of them.

History

Error correction techniques were developed to improve the accuracy on network analyzers calibration developing two main groups; those who use the twelve error term model: e.g. SOLT; and those who use the eight error term model: TRL, TRM, TRR, etc.

Short-Open-Line-Thru (SOLT) technique [26] uses the twelve error term model, making this technique useful for coaxial devices. The drawback of this technique is the use of standards that must be well known and specified.

The eight error term model based calibration techniques do not require the complete knowledge of the calibration elements e.g.: TRL. The TRL calibration technique [2] places the S parameter reference plane directly at the DUT. This calibration technique has the drawback of the Line standard because the multiples of 180° of the electric length of the lines lead to indetermination when computing the error estimation. The TRL standard is nowadays a reference for other calibration techniques.

Because of the TRL problem of the $180n°$ (where $n=\pm 1,2,\ldots,N$) electrical length difference, the National Institute of Standard and Technology (NIST) created the TRL multiline calibration technique [20]. This technique uses several lines in such a way that when a multiple of 180° electrical length difference occurs on one of them, other line corrects this error and so the line that provides the best estimation is chosen to correct the error boxes.

Several calibration techniques came later as improvements or alternatives to those techniques. The resulting parameters and the estimated errors help to extract the actual S parameters of the DUT. For the S parameters extraction, two methods exist: the classical method and the straight-forward method.

The straight-forward method for extracting the S parameters does not require moving the reference plane because the S parameters from the DUT are corrected directly and requiring partial computation of the error boxes, while the classical method requires complete computation of the error boxes.

Chapter 1

Characterization fundaments

This chapter covers the basis of the characterization of microwave devices using S parameters. S parameters bring direct information in the frequency domain about the reflected and incident waves of a Device Under Test (DUT). S parameters are measured with a Vector Network Analyzer (VNA), that has to be calibrated prior the measurements. Calibration is the process that eliminates the systematic errors of a VNA.

1.1 S-parameters

A two port network can be seen as a black box with one input and one output (Fig. 1.1). It can be characterized by means of Z, Y, ABCD or H parameters matrices. These matrices elements are obtained by using short and open circuit conditions and are suitable for low frequency devices characterization. However, at high frequencies the open and short circuit conditions become harder to accomplish and may produce instability of active devices. Thus, to overcome these problems, the scattering parameters (S parameters) matrix was developed[18].

The S parameter matrix provides a complete description of an N-port network (Gain, Isolation, Impedance, etc.). These parameters relates the incident wave at one port, to the reflected wave at that port and those transmitted to the rest of the ports. These S parameters can be measured directly with a VNA and once having them, conversion to other parameters can be made.

The incident voltage and current in a transmission line or a one port network can be modeled by (1.1) and (1.2)

$$V(x) = V^+(x) + V^-(x) \quad (1.1)$$

$$I(x) = I^+(x) - I^-(x) = \frac{V^+(x)}{Z_0} - \frac{V^-(x)}{Z_0} \quad (1.2)$$

where,

$$V^+ = Ae^{-j\beta x} \quad (1.3)$$

$$V^- = Be^{j\beta x} \quad (1.4)$$

Having computed the V^+ and V^-, The reflection coefficient is defined as the ratio of the reflected wave to the incident wave as (1.5)

$$\Gamma(x) = \frac{V^-(x)}{V^+(x)}. \quad (1.5)$$

In order to work with power waves, a normalized notation should be used [4]

$$v(x) = \frac{V(x)}{\sqrt{Z_0}} \quad (1.6)$$

$$i(x) = \sqrt{Z_0} I(x) \quad (1.7)$$

$$a(x) = \frac{V^+(x)}{\sqrt{Z_0}} \quad (1.8)$$

$$b(x) = \frac{V^-(x)}{\sqrt{Z_0}} \quad (1.9)$$

In that sense $v(x)$ and $i(x)$ can be written as follows:

$$v(x) = a(x) + b(x), \quad (1.10)$$

$$i(x) = a(x) - b(x). \quad (1.11)$$

And the reflection coefficient $\Gamma(x)$ in terms of incident and reflected power wave is now:

$$\Gamma(x) = \frac{b(x)}{a(x)} \quad (1.12)$$

From the definitions mentioned above, a normalized incident voltage wave $a(x)$ and a reflected wave $b(x)$ in terms of $V(x)$ and $I(x)$ can be represented as:

$$a(x) = \frac{1}{2}[v(x) + i(x)] = \frac{1}{2\sqrt{Z_0}}[V(x) + Z_0 I(x)] \quad (1.13)$$

$$b(x) = \frac{1}{2}[v(x) - i(x)] = \frac{1}{2\sqrt{Z_0}}[V(x) - Z_0 I(x)] \quad (1.14)$$

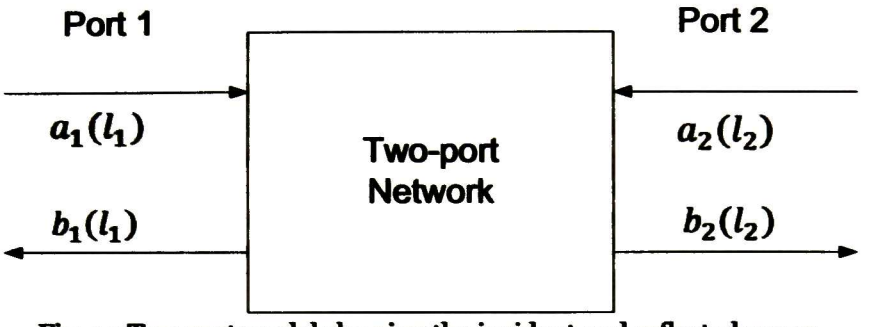

Fig. 1.1 Two port model showing the incident and reflected waves.

For a two port network (as shown in Fig. 1.1) where $a_n(l_n)$ is the amplitude of the incident power wave at port n and $b_n(l_n)$ represents the reflected power wave at the same port. Since $\Gamma(x)$ is defined as the ratio of reflected power wave to the incident power wave, a 2-port network can be represented in matrix form as:

$$\begin{bmatrix} b_1 \\ b_2 \end{bmatrix} = \begin{bmatrix} S_{11} & S_{12} \\ S_{21} & S_{22} \end{bmatrix} \begin{bmatrix} a_1 \\ a_2 \end{bmatrix} \quad (1.15)$$

where

- **S_{11} is the reflection coefficient at port 1,**

$$S_{11} = \left.\frac{b_1}{a_1}\right|_{a_2=0} \quad (1.16)$$

- **S_{22} is the reflection coefficient at port 2,**

$$S_{22} = \left.\frac{b_2}{a_2}\right|_{a_1=0} \quad (1.17)$$

- **S_{21} is the transmission coefficient from port 1 to port 2**

$$S_{21} = \left.\frac{b_2}{a_1}\right|_{a_2=0} \quad (1.18)$$

- **S_{12} is the transmission coefficient from port 2 to port 1**

$$S_{12} = \left.\frac{b_1}{a_2}\right|_{a_1=0} \quad (1.19)$$

For the general case of a N-port network, the S parameter matrix is as follows (1.20):

$$\begin{bmatrix} b_1(l_1) \\ b_2(l_2) \\ \vdots \\ b_N(l_N) \end{bmatrix} = \begin{bmatrix} S_{11}\, S_{12} \ldots S_{1N} \\ S_{21}\, S_{22} \ldots S_{2N} \\ \vdots \quad \vdots \quad \ddots \quad \vdots \\ S_{N1}\, S_{N2} \ldots S_{NN} \end{bmatrix} \begin{bmatrix} a_1(l_1) \\ a_2(l_2) \\ \vdots \\ a_N(l_N) \end{bmatrix} \quad (1.20)$$

For the special case of a two port network, parameters S_{11} and S_{21} are determined by measuring the magnitude and phase of the incident and reflected wave, when the output of port 2 is ended at Z_0 (normally 50 Ω). This condition ensures that any other port, different from the incident wave is matched avoiding incident waves entering from other ports as no reflections are present. The precision of the measurements depends largely on how good is the termination at the ports.

With the magnitude and phase information of the incident and reflected waves, it is possible to quantify the reflection and information of any DUT. The reflection and transmission characteristics can be expressed in vector (Magnitude and phase) or scalar (Magnitude only) form.

On one hand, the reflection coefficient data (S_{11} and S_{22}) are related with:

- Return loss.
- SWR (Standing Wave Ratio).
- Impedance and Admittance ($R + jX, G + jB$).

And on the other hand, the transmission coefficient data (S_{21} and S_{12}) are related with:

- Insertion Loss/Gain.
- Insertion Phase.
- Group Delay.
- Isolation.

1.2 Microstrip

RF circuits are normally fabricated on Printed Circuit Boards (PCBs) due to the easiness of manufacture and its low cost. In addition, traces of PCBs are extensively used to interconnect Radio Frequency Integrated Circuits (RFICs) and Monolithic Microwave Integrated Circuits (MMICs). At microwave frequencies, the traces must be modeled as transmission lines (See Fig. 1.2).

A PCB can be composed of several layers depending on its application. The simplest PCB layout consists of three layers; the bottom layer is the ground plane, the middle layer is the dielectric plane and the top layer is where the traces are located. The ground plane helps prevent excessive field leakage and thus reduces radiation loss. In any microstrip there exist field leakage; this leakage depends on the dielectric material and thickness.

The dielectric controls the electric field leakage, the severity of it, depends on the relative dielectric constant. High dielectric constant and low height dielectric helps to have less field leakage.

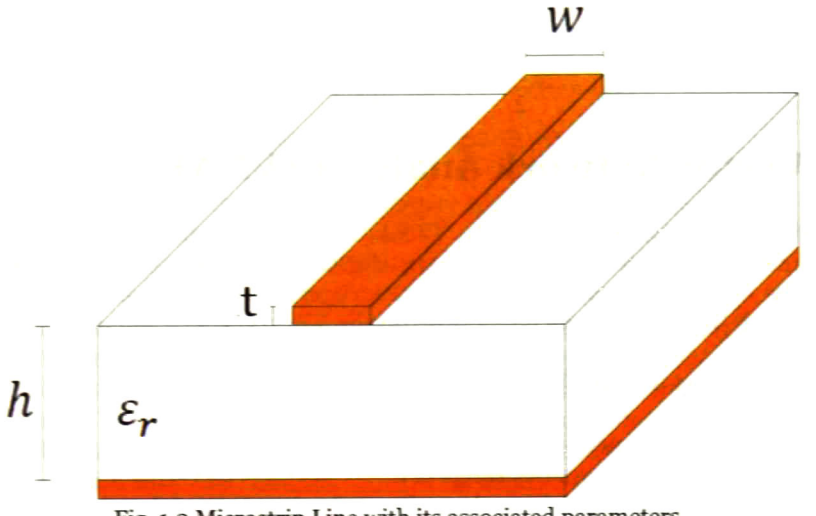

Fig. 1.2 Microstrip Line with its associated parameters.

Empirical formulas have been developed for microstrip transmission lines that suits the balance between complexity and accuracy. A first approximation, assumes that the thickness t of the conductor forming the trace is negligible compared to the substrate height h (i.e.: $t/h < 0.005$)[8]. In this case there are two regions of applicability depending on wether the ratio w/h is larger or less than unity.

According to Wheeler[19], for narrow strip lines, $w/h < 1$, the characteristic impedance of the line can be approximated by:

$$Z_0 = \frac{Z_f}{2\pi\sqrt{\varepsilon_{eff}}} \ln\left(8\frac{h}{w} + \frac{w}{4h}\right) \qquad (1.21)$$

where,

$$Z_f = \sqrt{\mu_0/\varepsilon_0} = 376.8\,\Omega \qquad (1.22)$$

which is the characteristic impedance in free space, ε_{eff} is the effective dielectric constant given by

$$\varepsilon_{eff} = \frac{\varepsilon_r + 1}{2} + \frac{\varepsilon_r - 1}{2}\left[\left(1 + 12\frac{h}{w}\right)^{-1/2} + 0.04\left(1 - \frac{w}{h}\right)^2\right] \qquad (1.23)$$

For a wide line, $w/h > 1$, we need to use a different formula that computes the characteristic impedance of the line

$$Z_0 = \frac{Z_f}{\sqrt{\varepsilon_{eff}}\left(1.393 + \frac{w}{h} + \frac{2}{3}\ln\left(\frac{w}{h} + 1.444\right)\right)} \quad (1.24)$$

with

$$\varepsilon_{eff} = \frac{\varepsilon_r + 1}{2} + \frac{\varepsilon_r - 1}{2}\left(1 + 12\frac{h}{w}\right)^{-1/2} \quad (1.25)$$

1.3 Vector Network Analyzer (VNA)

The Vector Network Analyzer (VNA) is a measurement equipment that measures the S-parameters of any device at high frequencies, measuring the magnitude and phase of the reflection and transmission coefficients. Normally it has 2 or 4 ports depending on the VNA type.

The VNA consist of (See Fig. 1.3):

- **The RF-source:** is a programmable sweep tuner, which goes through the specified frequency range [1].
- **The test set:** is where the split of the incident and reflected wave is made, by means of directional couplers and power splitters.
- **The receiver:** It furnishes the medium to detect and convert the RF/microwave signals into lower frequencies.
- **The analyzer:** Once the RF/microwave signal has been detected, the network analyzer must process the signal to store and display the data.

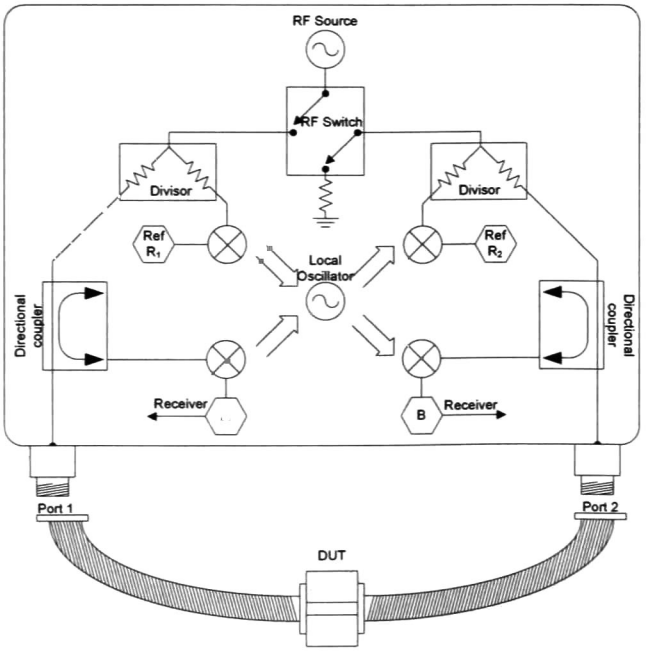

Fig. 1.3 VNA Basic block diagram

The VNA is a receiver; this means that the microwave signal is down converted into an intermediate frequency (IF) in order to compute the S parameter, as shown in Fig. 1.3. Basically, the RF signal is divided by the splitter, one branch is used as the signal reference while the other branch is sent to the DUT and the reflected wave is measured by the directional coupler located at the DUT branch. Thus, from this principle the S parameters are measured.

In polar form, S-parameters provide essential information about the DUT suitable to:

- Fully characterizes any device in terms of power ratios.
- Design efficient matching networks.
- Developing accurate models require magnitude and phase.

1.3.1 VNA measurement considerations

By just measuring a DUT S parameters from the VNA is not enough. In order to get useful measurements, some considerations have to be taken into account due to the errors in the VNA measurements. They are due to the non-ideality of the internal VNA components and external sources that contaminates the signal sent from the VNA to the DUT. Some errors can be controlled and some cannot because they are random. This work focuses of only one type of errors: the systematic errors. The different types of errors are:

- **Systematic errors:** As frequency increases, undesirable effects appear due to the non-ideality of the VNA components (e.g.: directivity, frequency response, decoupling, attenuators, switches, etc.).
- **Random errors:** These errors vary randomly as a function of time, as they are not predictable, they cannot be removed by calibration.
- **Environmental errors:** The environmental errors occur when the test set conditions change after a calibration has been made (e.g.: temperature change).

On the characterization of non-coaxial devices (e.g.: coplanar, microstrip) a mechanical support is used to mount the DUT, as these devices cannot be connected directly to the VNA. The test fixture dimensions and topology depend upon the dimensions of the non-coaxial device that is to be measured.

For a coplanar technology of small size, a probe station is used and for microstrip technology a test fixture is used. By using these mechanical supports, the measurement becomes prone to more errors and losses, so care should be taken to avoid changes in measurements. Transitions that help us as interface to connect the DUT and adapt it to the coaxial connectors of the VNA always are accompanied by dispersion, attenuation or both. For the added errors of the mechanical support and the systematic errors, calibration techniques have been developed to eliminate them from the measurements.

Error correction is a mathematical process where systematic errors are modeled and estimated.

The error estimation mentioned above can be made in one or two stages. The error correction techniques are divided in two groups:

- **One Stage Calibration (One Tier):** Errors are estimated and eliminated from the VNA and from the test fixture during the same process utilizing auto-calibration technique (e.g.: TRL, TRM, TAR, TRRM, etc.). These techniques neglect the isolating errors between ports and the errors caused by the switch position change.
- **Two Stage Calibration (Two Tier):** On the first stage VNA systematic errors are estimated (including isolating and switching errors) by the SOLT calibration technique for coaxial devices. On the second stage test fixture errors are estimated with an auto-calibration technique.

The systematic errors are determined by the difference between measured data and the known response to the calibration standards. Systematic errors can be modeled by flow diagrams. There exist one port error model and two port error models, depending on the number of ports and the errors taken into consideration.

1.3.2 Test Fixture

The test fixture is a mechanical support that mount the calibration standards and the DUT (See Fig. 1.4). The ideal test fixture has the following characteristics [7]:

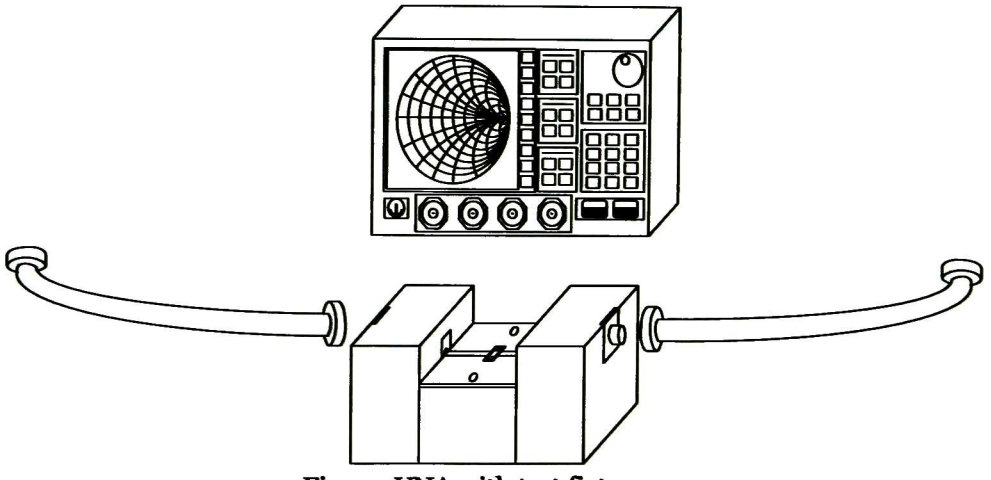

Fig. 1.4 VNA with test fixture

- No loss and no electrical length.
- Flat frequency response.
- Perfect impedance match between the test system and DUT ports.
- No crosstalk between the fixture's input and output ports.
- Fast, easy, repeatable connections.

Each of the characteristics explained above are met by:

- Keeping the amount of loss and phase errors of the test fixture less than the system's measurement uncertainty.
- Making sure that the DUT bandwidth is less than fixture bandwidth.
- Ensure that the characteristic impedance Z_0 of the test system is equal to that of the test fixture Z_T ($Z_0 = Z_T$).
- The test fixture crosstalk has to be less than the loss or isolation of the DUT.
- The measurement has to have repeatability.

Errors and DUT, when measured by the VNA can be modeled by flow graph theory depending on the number of ports and errors.

1.4 Signal Flow graph theory

Signal flow graph is a useful technique for the analysis of microwave networks in terms of transmitted and reflected waves. It is commonly used in system and control theory. The signal flow graph is composed of branches (directed paths) and nodes connecting these paths:

- Nodes: they are the end points of a directed segment. They identify network parameters such as a_1, b_1, a_2, b_2 when dealing with S parameters.
- Branches: is a directed path between two nodes, representing signal flow from one node to another.

The technique is useful because it provides a graphical representation of a microwave network, allowing for a qualitative analysis and interpretation of the network. In addition it provides a method for simplifying a microwave network to a more fundamental form (networks are reduced to input-output relations). Table 1.1 shows the basic identities that help solving the error models by signal flow graph theory

1.5 Error models

Error models computed with signal flow graph theory help finding the error coefficients needed in order to solve for the S parameters of the DUT, this is the principle of the calibration. Obtaining a reliable calibration technique based on construction and cost effectiveness is the goal.

The perfect VNA has infinite isolation between ports, infinite directivity, no impedance mismatches anywhere, and a flat frequency response. In practice, the VNA's internal components are non-ideal. Definitions of what it was stated is shown next:

Directivity: is a measure of how well the VNA's couplers separate the forward and reflected waves. High value of directivity is desirable.

Source match: is how closely the path of the source matches Z_0.

Load match: is the quality of the path of the load termination.

Both matches can be impacted by discontinuities between the RF source and the sampling paths.

Frequency response tracking: is how well the magnitude and phase of a signal passing through the VNA compares to the reference signal.

Transmission mismatch: is due to impedance mismatch between the test ports of the system and the ports of the DUT.

Isolation: is the leakage of energy between the test and reference channels inside the VNA. Leakage between the transmitted and reflected paths within the VNA contaminates low-level signals.

Nodal Assignment	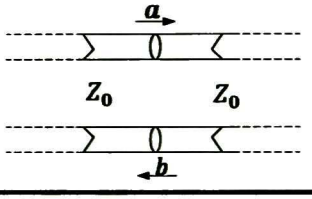	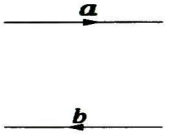
Branch	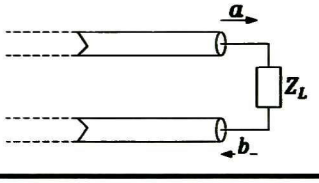	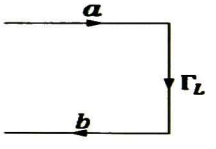
Series Connection	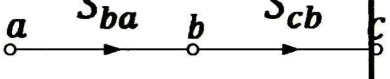	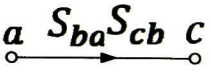
Parallel Connection	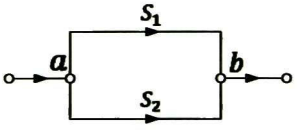	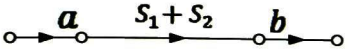
Splitting of Branches	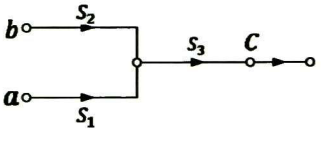	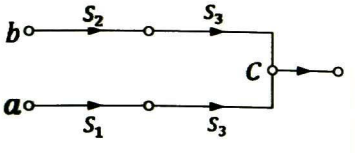
Self-loop	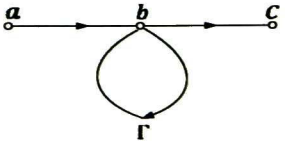	

Table 1.1 The signal flow graphs and its equivalences or reductions.

1.6.1 Error model for one port.

The one-port error model is useful for measuring reflection coefficient of the DUT. In that sense the VNA is modeled with an ideal reflectometer (i.e.: lossless, matched and without frequency response errors) and a fictitious error adapter, as shown in Fig. 1.5, where the DUT is represented with a reflection coefficient Γ_L, while the reflection coefficient measured by the VNA is represented as Γ_{meas}.

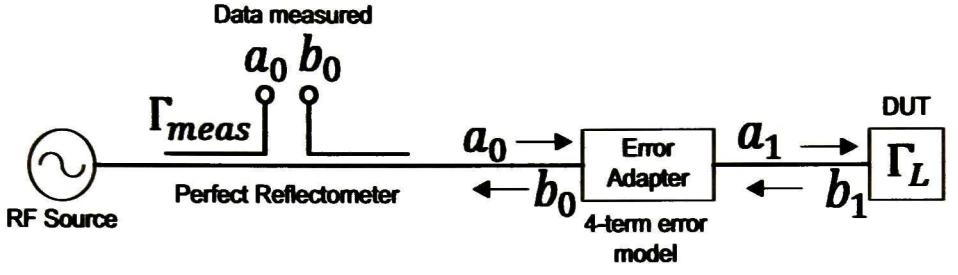

Fig. 1.5 One-port error model

The fictitious error adapter for one-port contains 4 error terms e_{00}, e_{11}, e_{01} and e_{10}. Fig. 1.6 shows the flow graph diagram that represents the one-port error model.

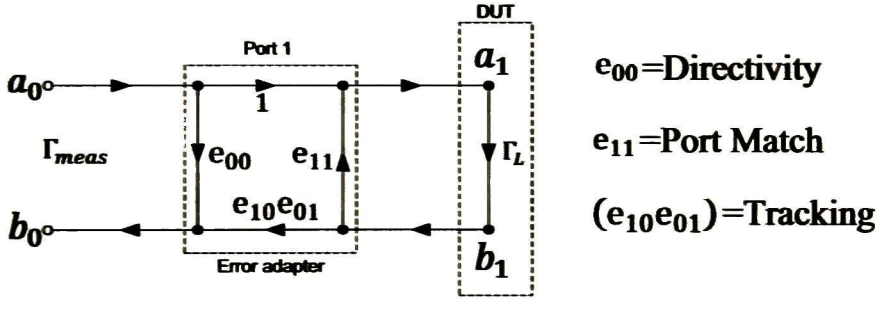

Fig. 1.6 Flow graph diagram representation for the One-port error model

One-port calibration allows measurement and elimination of three systematic error terms: directivity (e_{00}), source coupling (Port Match) (e_{11}) and frequency response (Tracking) ($e_{10}e_{01}$). These three error terms are derived, that is, solved in terms of three simultaneous equations.

In order to establish these equations, three known calibration standards are measured to estimate the errors (e.g.: Short, Open and Load). The Load impedance has to be the same as the characteristic impedance of the system (Z_0). Solving the equations, the systematic errors are found and then a derivation of the real S parameters is found.

The mathematical procedure, described in the last paragraph, is explained in detail from (1.26)-(1.28). By means of Mason's rule and the equivalences of flow graph theory explained back in section 1.4, the measured reflection coefficient Γ_{meas} from Fig. 1.6 is expressed as:

$$\Gamma_{meas} = \frac{b_0}{a_0} = e_{00} + \frac{e_{01}e_{10}\Gamma_L}{1 - e_{11}\Gamma_L} \quad (1.26)$$

thus Γ_L is

$$\Gamma_L = \frac{\Gamma_{meas} - e_{00}}{(e_{01}e_{10} - e_{00}e_{11}) + e_{11}\Gamma_{meas}} \quad (1.27)$$

In order to obtain the real reflection coefficient Γ_L of the DUT, it is needed to determine the error terms e_{00}, e_{11}, e_{10} and e_{01}. Therefore, by convenience Γ_{meas} can be written as shown in (1.28):

$$\Gamma_{meas} = \frac{e_{00} + \Gamma_L(e_{01}e_{10} - e_{00}e_{11})}{1 - \Gamma_L e_{11}} \quad (1.28)$$

Rearranging terms of eq. (1.28), Γ_{meas} is found to be:

$$\Gamma_{meas} = b + \Gamma_L a - \Gamma_{meas}\Gamma_L c \quad (1.29)$$

where,

$$b = e_{00}$$

$$c = -e_{11}$$

$$a = (e_{01}e_{10} - e_{00}e_{11})$$

Evaluating the coefficients a, b, c from eq. (1.29), requires three different known values Γ_L: Short (Γ_L^{Short}), Open (Γ_L^{Open}) and Load (Γ_L^{Load}). Hence, three equations are obtained

$$\Gamma_{meas}^{short} = b + \Gamma_L^{short} a - \Gamma_{meas}^{short}\Gamma_L^{short} c \quad (1.30)$$

$$\Gamma_{meas}^{open} = b + \Gamma_L^{open} a - \Gamma_{meas}^{open}\Gamma_L^{open} c \quad (1.31)$$

$$\Gamma_{meas}^{load} = b + \Gamma_L^{load} a - \Gamma_{meas}^{load}\Gamma_L^{load} c \quad (1.32)$$

where Γ_L^{short}, Γ_L^{open} and Γ_L^{load} are defined as

$$\Gamma_L^{short} = -e^{-2\gamma l} \quad (1.33)$$

$$\Gamma_L^{open} = e^{-2\gamma l} \quad (1.34)$$

$$\Gamma_L^{Load} = 0 \quad (1.35)$$

Notice that γ and l are the propagation constant and the physical length of the reflect respectively. Substituting (1.33)-(1.35) into (1.30)-(1.32) it is obtained

$$\Gamma_{meas}^{short} = b - e^{-2\gamma l}a - \Gamma_{meas}^{short}e^{-2\gamma l}c \quad (1.36)$$

$$\Gamma_{meas}^{open} = b + e^{-2\gamma l}a + \Gamma_{meas}^{open}e^{-2\gamma l}c \quad (1.37)$$

$$\Gamma_{meas}^{load} = b \quad (1.38)$$

(1.36)-(1.38) can be expressed in matrix form as shown in (1.39)

$$\begin{bmatrix} \Gamma_{meas}^{short} \\ \Gamma_{meas}^{open} \\ \Gamma_{meas}^{load} \end{bmatrix} = \begin{bmatrix} 1 & -e^{-2\gamma l} & -\Gamma_{meas}^{short}e^{-2\gamma l} \\ 1 & e^{-2\gamma l} & \Gamma_{meas}^{open}e^{-2\gamma l} \\ 1 & 0 & 0 \end{bmatrix} \begin{bmatrix} b \\ a \\ c \end{bmatrix} \quad (1.39)$$

1.6.2 Error model for two ports.

Error models for two ports are for measuring transmission and reflection coefficients. There exist two error models: the 12-term and 8-term error model. The 12-term error model takes more errors into account, thus being more accurate. The 8-term error model neglects the isolation and the load coupling becomes a source coupling reducing the errors from the 12-term error model.

1.6.2.1 twelve term error model for two ports.

Principal sources of systematic errors are considered for the two port error correction. Based on the one port error model, the 12-term error model can be calculated.

The VNA is modeled as shown in Fig. 1.7. A reflectometer is placed at the input of the network. It is be modeled ideally cascaded to a fictitious error adapter for port 1 and 2 respectively. A switch changes the direction from the RF source to the unknown network ending with an impedance equals to the characteristic impedance Z_0 utilized in the system, the switch has two positions: one for forward sense and the other for the reverse sense. When the source is connected in forward sense, the output of the network is matched at Z_0 impedance and conversely for the reverse sense.

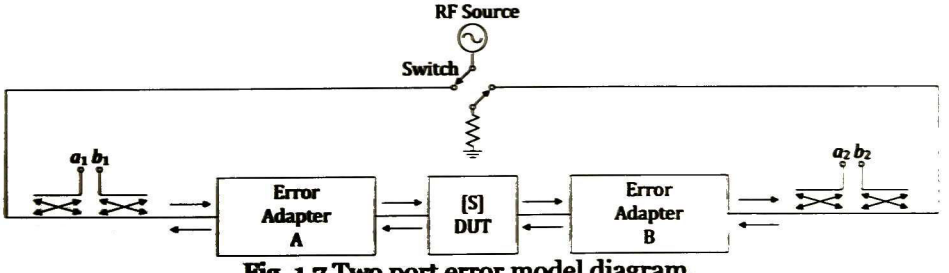

Fig. 1.7 Two port error model diagram.

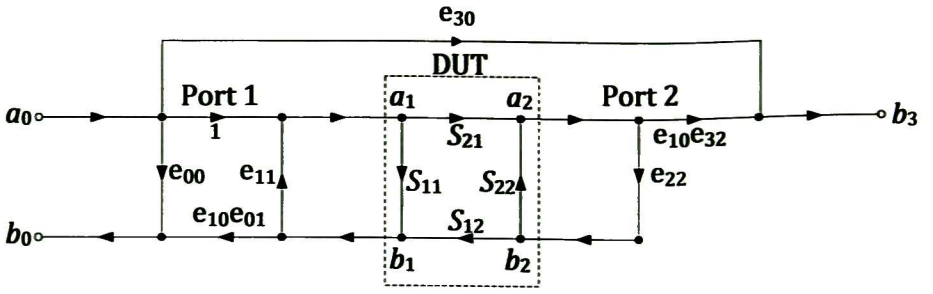

Fig. 1.8 Error model in forward sense.

A twelve term error model is shown in Fig. 1.8 and Fig. 1.9. The six systematic errors in the forward sense are [14]

e_{00} = Directivity. $e_{10}e_{32}$ = Frequency response in transmission

e_{11} = Source coupling $e_{10}e_{01}$ = Frequency response in reflection

e_{22} = Load coupling e_{30} = Isolation

Solving the flow diagram in forward sense (Fig. 1.8), the measured S-parameters S_{11M} and S_{21M} can be computed. These two parameters depend on the real four S-parameters of the DUT along with six error terms.

$$S_{11M} = \frac{B_0}{A_0} = e_{00} + (e_{10}e_{01})\frac{S_{11} - e_{22}\Delta_S}{1 - e_{11}S_{11} - e_{22}S_{22} + e_{11}e_{22}\Delta_S} \qquad (1.40)$$

$$S_{21M} = \frac{B_3}{A_0} = e_{30} + (e_{10}e_{32})\frac{S_{21}}{1 - e_{11}S_{11} - e_{22}S_{22} + e_{11}e_{22}\Delta_S} \qquad (1.41)$$

where

$$\Delta_S = S_{11}S_{22} - S_{21}S_{12}$$

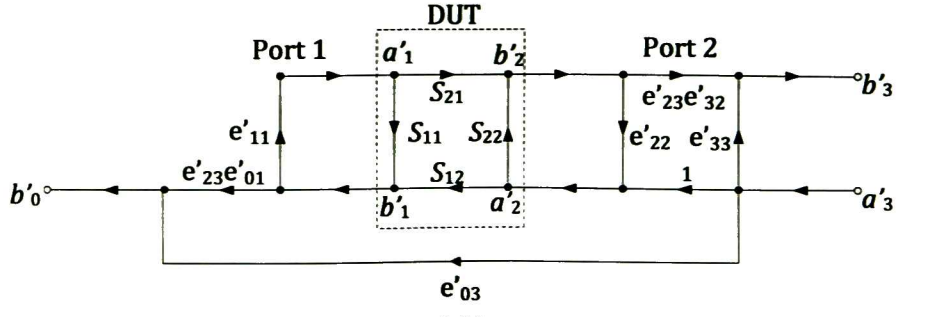

Fig. 1.9 Error model in reverse sense.

Also, solving the diagram for the inverse sense (Fig. 1.9), the measured S parameters S_{22M} and S_{12M} are obtained. These two equations also depend on the four real S-parameters of the DUT along with other six error terms.

$$S_{22M} = \frac{B'_3}{A'_3} = e'_{33} + (e'_{23}e'_{32})\frac{S_{22} - e'_{11}\Delta_S}{1 - e'_{11}S_{11} - e'_{22}S_{22} + e'_{11}e'_{22}\Delta_S} \qquad (1.42)$$

$$S_{12M} = \frac{B'_0}{A'_3} = e'_{03} + (e'_{23}e'_{01})\frac{S_{12}}{1 - e'_{11}S_{11} - e'_{22}S_{22} + e'_{11}e'_{22}\Delta_S} \qquad (1.43)$$

the terms in reverse sense are

e'_{33} = Directivity

e'_{11} = Source coupling

e'_{22} = Load coupling

$e'_{23}e'_{01}$ = Frequency response in transmission

$e'_{23}e'_{32}$ = Frequency response in reflection

e'_{03} = Isolation

1.6.2.2 Eight term error model for two ports

The eight term error model for two port calibration is shown in Fig. 1.10. The error model used for calibration can be simplified to eight error terms due to the isolation and load coupling are neglected [13]. Hence eight measurements have to be made in order to compute the error terms.

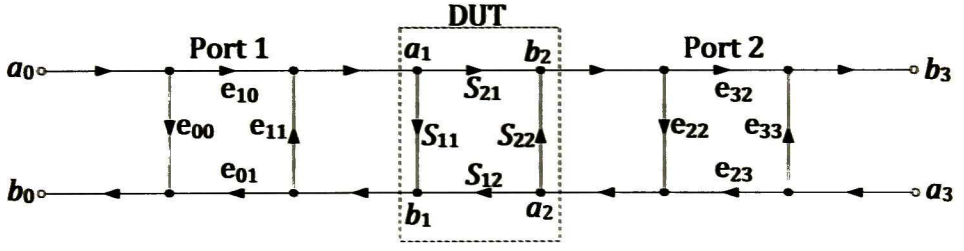

Fig. 1.10 Eight-term error model

4 error terms in forward sense

e_{00} = Directivity

e_{11} = Source coupling

$e_{10}e_{32}$ = Frequency response in transmission

$e_{10}e_{01}$ = Frequency response in reflection

4 error terms in reverse sense

e_{33} = Directivity

e_{22} = Source coupling

$e_{23}e_{32}$ = Frequency response in reflection

$e_{23}e_{01}$ = Frequency response in transmission

Chapter 2

Error Correction

This chapter will focus on the VNA errors that affect the measurements. These errors come principally from non-idealities from the components that are part of the VNA (i.e.: Test set, directional couplers, receivers, local oscillators, cables, test fixture, etc.).

Calibration techniques were developed to overcome such problems by estimating and eliminating the systematic errors, mathematically, this is known as error correction. This chapter will explain several calibration techniques (SOLT, TRL and LRRM). It should be noticed that there are more calibration techniques.

The SOLT and TRL calibration techniques serve as the basis to explain the LRRM calibration technique proposed in this work.

2.1 Switching errors

As commented earlier S-parameters of a two port network DUT are the power ratio of the incident and reflected waves when the ports are matched to Z_0. Even though the ports are matched to Z_0, ripples at high frequencies are observed due to decoupling of the source and the load Z_0 from the system (unmatched errors), this fact is known as switching errors. Switching errors correction is the first step that should be eliminated before the VNA calibration is done, this will eliminate the ripples seen on the measurements at high frequencies.

In Fig. 2.1b the terms a_3 and a_0 in reverse direction are the switching errors due to the decoupling of the source which ideally must be zero. In order to remove the switching errors from the measured S-parameters in any two-port device,

measurements of a_0, b_0, a_3, b_3 are made in both positions: forward and reverse mode.

- **Forward direction:** the microwave source generator and the load are connected through a switch to the points 1 and 2 respectively. At this position parameters a_0, b_0, a_3, b_3 are measured (Fig. 2.1a). S_{11} and S_{21} are normally measured in this configuration.

- **Reverse direction:** the microwave source generator and the load are connected through the switch to the points 2 and 1 respectively. At this position parameters a'_0, b'_0, a'_3, b'_3 are measured (Fig. 2.1b). S_{22} and S_{12} are normally measured in this configuration.

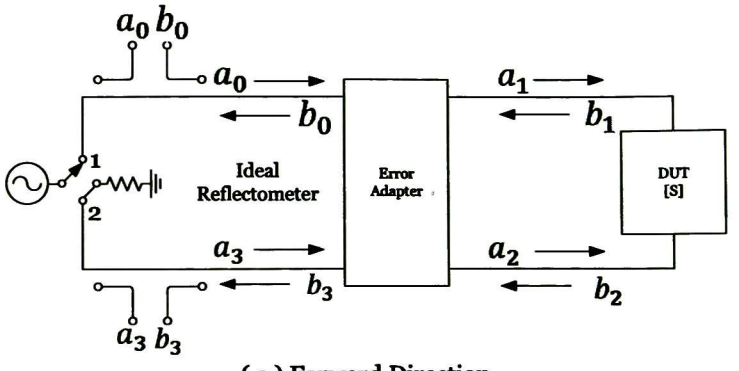

(a) Forward Direction

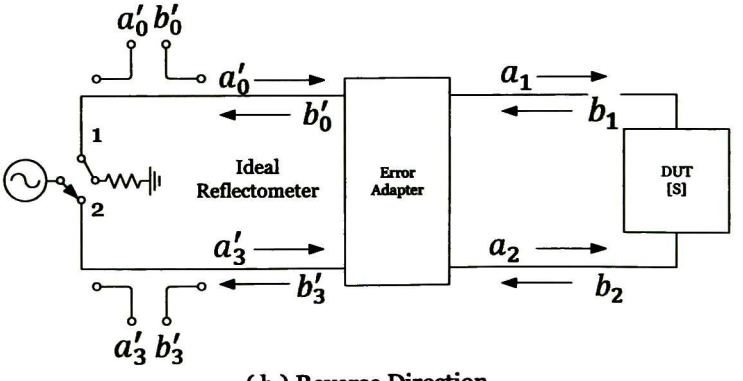

(b) Reverse Direction

Fig. 2.1 VNA diagram for switching errors.

When the source is at position 1 (forward direction), the measured S-parameters (S_{meas}) are expressed in matrix form by means of a_i and b_i (where $i = 0, 3$)

$$\begin{bmatrix} b_0 \\ b_3 \end{bmatrix} = \begin{bmatrix} S_{11meas} & S_{12meas} \\ S_{21meas} & S_{22meas} \end{bmatrix} \begin{bmatrix} a_0 \\ a_3 \end{bmatrix} \quad (2.1)$$

Conversely when the source is connected on position 2 (reverse direction), the S-parameters (S_{meas}) are expressed in matrix form by means of a'_i and b'_i (where $i = 0, 3$)

$$\begin{bmatrix} b_0' \\ b_3' \end{bmatrix} = \begin{bmatrix} S_{11meas} & S_{12meas} \\ S_{21meas} & S_{22meas} \end{bmatrix} \begin{bmatrix} a_0' \\ a_3' \end{bmatrix} \quad (2.2)$$

combining eq. (2.1) and eq. (2.2), measured S parameters are found:

$$\begin{bmatrix} b_0 & b_0' \\ b_3 & b_3' \end{bmatrix} = \begin{bmatrix} S_{11meas} & S_{12meas} \\ S_{21meas} & S_{22meas} \end{bmatrix} \begin{bmatrix} a_0 & a_0' \\ a_3 & a_3' \end{bmatrix} \quad (2.3)$$

$$\begin{bmatrix} S_{11meas} & S_{12meas} \\ S_{21meas} & S_{22meas} \end{bmatrix} = \begin{bmatrix} b_0 & b_0' \\ b_3 & b_3' \end{bmatrix} \begin{bmatrix} a_0 & a_0' \\ a_3 & a_3' \end{bmatrix}^{-1} \quad (2.4)$$

Eq. (2.4) helps us to eliminate the source and load unmatching errors presented in the measured S-parameters (S_{meas}) to any two-port network. From eq. (2.4) the measured S parameters without switching errors are shown in Table 2.1. For the switching error correction expressions are obtained where eight measurements are made.

$S_{11meas} = \dfrac{\frac{b_0}{a_0} - \frac{b_0'}{a_3'}\frac{a_3}{a_0}}{d}$	Forward Direction
$S_{21meas} = \dfrac{\frac{b_3}{a_0} - \frac{b_3'}{a_3'}\frac{a_3}{a_0}}{d}$	Forward Direction
$S_{12meas} = \dfrac{\frac{b_0'}{a_3'} - \frac{b_0}{a_0}\frac{a_0'}{a_3'}}{d}$	Reverse Direction
$S_{22meas} = \dfrac{\frac{b_3'}{a_3'} - \frac{b_3}{a_0}\frac{a_0'}{a_3'}}{d}$	Reverse Direction

Table 2.1 S-parameters switching errors free using eight measurements.

where

$$d = 1 - \frac{a_0'}{a_3'}\frac{a_3}{a_0}$$

2.2 Two port calibration

The VNA systematic errors can be modeled by two error adapters (Error boxes). Typically Port A and B Errors are contained within the error boxes, however, Transition, Test Fixture, Cables, etc. (Accessories) could be considered as part of the error boxes as well (see Fig. 2.2).

In order to estimate and eliminate these errors, a calibration process must be made. Several calibration techniques have been proposed in the literature,

their complexity, accuracy and cost will depend on the needs and resources, the calibration techniques are divided in two main groups:

- Standard calibration technique
  - SOLT (Short, Open, Load, Thru)

  Auto-calibration technique
  - LRL (Line, Reflect, Line)
  - LRRM (Line, Reflect, Reflect, Match)
  - LAR (Line, Attenuator, Reflect)

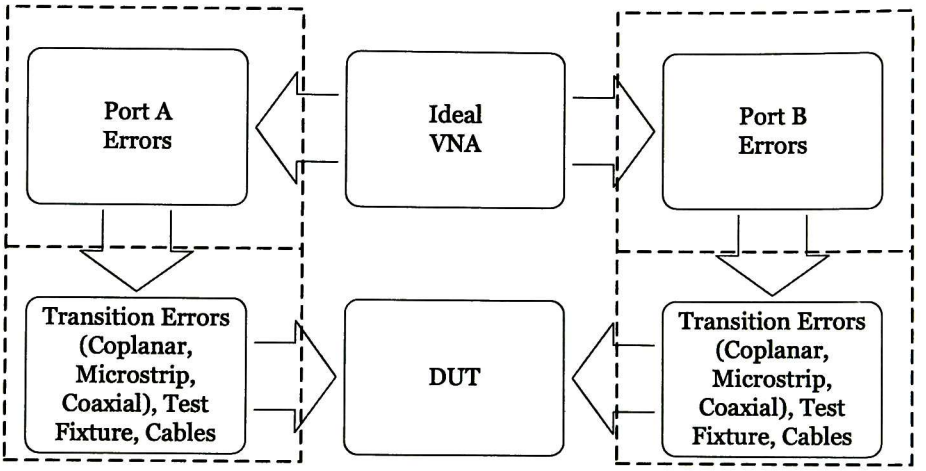

Fig. 2.2 Microwave measurement system block diagram based on a VNA.

In the SOLT calibration technique all standards must be completely known, on the other hand the other techniques, only require a partial knowledge of the standards. It is worth to mention that the error box coefficients depend on the quality of the standards being used.

Calibration techniques LRL, LRM and LAR are an alternative to the SOLT calibration technique, because, they are suitable, simpler and convenient when measuring non-coaxial devices, such as; devices that are mounted on a test fixture or in coplanar devices that can be characterized by a test probe station. Another advantage for these calibration techniques is that they only use three standards for their characterization with respect to the four standards used by the SOLT, moreover, Standards of the TRL calibration technique are less rigorous and easier to fabricate.

2.2.1 Short-Open-Load-Thru (SOLT) Calibration Technique

SOLT technique is one of the most used techniques for coaxial devices, normally is the calibration technique that comes embedded in the VNA firmware. The measured S parameters are based on the 12 term error model (Recall Section 1.6.2.1):

$$S_{11MEAS} = e_{00} + (e_{10}e_{01})\frac{S_{11} - e_{22}\Delta S}{1 - e_{11}S_{11} - e_{22}S_{22} + e_{11}e_{22}\Delta S} \quad (2.5)$$

$$S_{21MEAS} = e_{30} + (e_{10}e_{32})\frac{S_{21}}{1 - e_{11}S_{11} - e_{22}S_{22} + e_{11}e_{22}\Delta S} \quad (2.6)$$

$$S_{22MEAS} = e'_{33} + (e'_{23}e'_{32})\frac{S_{22} - e'_{11}\Delta S}{1 - e'_{11}S_{11} - e'_{22}S_{22} + e'_{11}e'_{22}\Delta S} \quad (2.7)$$

$$S_{12MEAS} = e'_{03} + (e'_{23}e'_{32})\frac{S_{12}}{1 - e'_{11}S_{11}e'_{22}S_{22} + e'_{11}e'_{22}\Delta S} \quad (2.8)$$

where

$$\Delta S = S_{11}S_{22} - S_{21}S_{12}$$

According to the one port error model, some error coefficients of eq. (2.5) (2.8) can be computed by using the Short, Open and Load standards and so the error boxes (shown in Fig. 2.2 Port A and B Errors).

Recalling from section 1.6.1 the error coefficients for error box A is:

$$\begin{bmatrix} b \\ a \\ c \end{bmatrix} = \begin{bmatrix} 1 & -e^{-2\gamma l} & -\Gamma_{meas}^{short} e^{-2\gamma l} \\ 1 & e^{-2\gamma l} & \Gamma_{meas}^{open} e^{-2\gamma l} \\ 1 & 0 & 0 \end{bmatrix}^{-1} \begin{bmatrix} \Gamma_{meas}^{short} \\ \Gamma_{meas}^{open} \\ \Gamma_{meas}^{load} \end{bmatrix}$$

for port B

$$\begin{bmatrix} \varphi \\ \alpha \\ \beta \end{bmatrix} = \begin{bmatrix} 1 & -e^{-2\gamma l} & -\Gamma_{meas}^{short} e^{-2\gamma l} \\ 1 & e^{-2\gamma l} & \Gamma_{meas}^{open} e^{-2\gamma l} \\ 1 & 0 & 0 \end{bmatrix}^{-1} \begin{bmatrix} \Gamma_{meas}^{short} \\ \Gamma_{meas}^{open} \\ \Gamma_{meas}^{load} \end{bmatrix}$$

where

$$-\varphi = e'_{33}$$

$$\beta = e'_{22}$$

$$\alpha = e'_{32}e'_{23} - e'_{22}e'_{33}$$

The leakage or crosstalk errors are computed from the 12 error term model from section 1.6.2.1 by placing a match (Z_0) at each port [14] making $S_{11} = S_{22} = S_{12} = S_{21} = 0$ and resulting in the e_{30} and e'_{03} error terms. There are still four more variables left to compute (e_{22}, $e_{10}e_{32}$, e'_{11} and $e'_{23}e'_{01}$).

Connecting a short length line between the ports, $S_{11} = S_{22} = 0$ and $S_{21} = S_{12} = 1$ and the e_{22} can be found in forward mode

$$e_{22} = \frac{S_{11MEAS} - e_{00}}{(e_{11}S_{11MEAS} - \Delta e)} \quad (2.9)$$

$$e_{10}e_{32} = (S_{21MEAS} - e_{30})(1 - e_{11}e_{22}) \quad (2.10)$$

while e'_{11} can be found in reverse mode as

$$e'_{11} = \frac{S_{22MEAS} - e'_{33}}{S_{22MEAS}e'_{22} - \Delta e'} \quad (2.11)$$

$$e'_{23}e'_{01} = (S_{12MEAS} - e'_{03})(1 - e'_{11}e'_{22}) \quad (2.12)$$

Once the 12 error terms are computed, the real S parameters are

$$S_{11} = \frac{\left(\frac{S_{11M} - e_{00}}{e_{10}e_{01}}\right)\left[1 + \left(\frac{S_{22M} - e'_{33}}{e'_{23}e'_{32}}\right)e'_{22}\right] - e_{22}A}{D} \quad (2.13)$$

$$S_{21} = \frac{\left(\frac{S_{21M} - e_{30}}{e_{10}e_{32}}\right)\left[1 + \left(\frac{S_{22M} - e'_{33}}{e'_{23}e'_{32}}\right)(e'_{22} - e_{22})\right]}{D} \quad (2.14)$$

$$S_{12} = \frac{\left(\frac{S_{12M} - e'_{03}}{e'_{23}e'_{01}}\right)\left[1 + \left(\frac{S_{11M} - e_{00}}{e_{10}e_{01}}\right)(e_{11} - e'_{11})\right]}{D} \quad (2.15)$$

$$S_{22} = \frac{\left(\frac{S_{22M} - e'_{33}}{e'_{23}e'_{01}}\right)\left[1 + \left(\frac{S_{11M} - e_{00}}{e_{10}e_{01}}\right)e_{11}\right] - e'_{11}A}{D} \quad (2.16)$$

where

$$D = \left[1 + \left(\frac{S_{11M} - e_{00}}{e_{10}e_{01}}\right)e_{11}\right]\left[1 + \left(\frac{S_{22M} - e'_{33}}{e'_{23}e'_{32}}\right)e'_{22}\right] - Ae_{22}e'_{11} \quad (2.17)$$

$$A = \left(\frac{S_{21M} - e_{30}}{e_{10}e_{32}}\right)\left(\frac{S_{12M} - e'_{03}}{e'_{23}e'_{01}}\right)$$

2.2.2 Thru-Reflect-Line (TRL) Calibration Technique

The TRL has been a reference calibration technique and was developed by Engen & Hoer[2]. This technique allows computing the VNA systematic errors. In [11] an improvement to the TRL technique was proposed, where the lengths of the lines are not necessary known and neither the propagation constant (γ) in order to determine the S parameters of the DUT.

The TRL needs three standards

- Two non-reflecting transmission lines (i.e.: L_{REF} and L_2): L_{REF} as the reference line (also known as Thru).
- A symmetric transmission line ended with a high reflection coefficient in magnitude (i.e.: Reflect): it can be either an open or a short circuit.

For non-coaxial devices the DUT must be mounted on a mechanical support called Test Fixture, that it is the transition from coaxial to microstrip technology. The TRL calibration technique estimates the systematic errors that are intrinsic to the VNA and the test fixture. Once the VNA is calibrated, one can proceed to measure the DUT and obtain its actual S parameters.

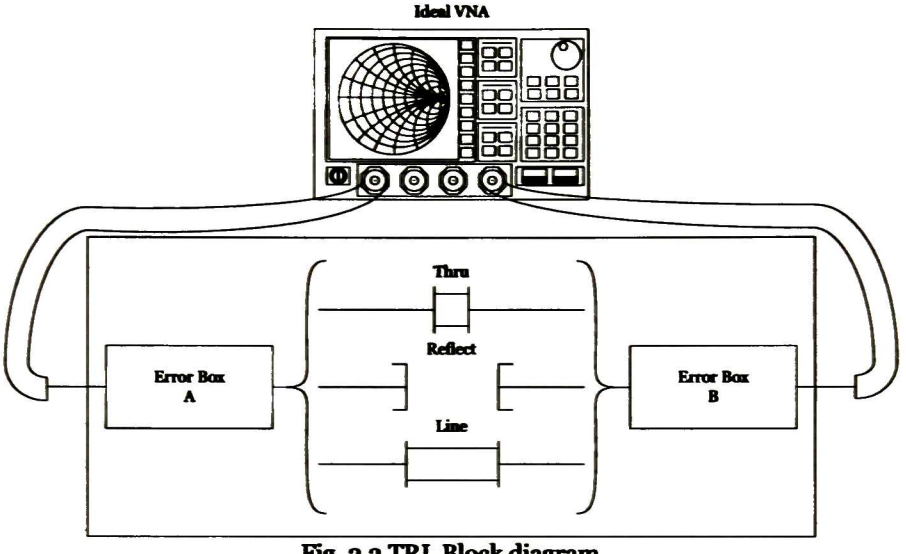

Fig. 2.3 TRL Block diagram.

From Fig. 2.3 it is seen that the error boxes are connected in cascade form to the standards and the DUT. Exploiting the properties of the wave cascade matrix, the S parameters of the networks connected in cascade can be derived. The wave cascade matrix (also known as, T parameters) are defined as

$$T = \frac{1}{S_{21}}\begin{bmatrix} -\Delta_S & S_{11} \\ -S_{22} & 1 \end{bmatrix} \tag{2.18}$$

Generally speaking, the measured wave cascade matrix of the error boxes and any network connected to the VNA can be represented as

$$T_C = T_A T_N T_B \tag{2.19}$$

where

$$T_A = \frac{1}{e_{01}}\begin{bmatrix} -(e_{00}e_{11} - e_{01}e_{10}) & e_{00} \\ -e_{11} & 1 \end{bmatrix} = r_{22}\begin{bmatrix} a & b \\ c & 1 \end{bmatrix} \tag{2.20}$$

$$T_N = \begin{bmatrix} t_{N11} & t_{N12} \\ t_{N21} & t_{N22} \end{bmatrix} \tag{2.21}$$

$$T_B = \frac{1}{e_{32}}\begin{bmatrix} -(e_{23}e_{32} - e_{22}e_{33}) & e_{22} \\ -e_{33} & 1 \end{bmatrix} = \rho_{22}\begin{bmatrix} \alpha & \beta \\ \varphi & 1 \end{bmatrix} \tag{2.22}$$

Once the networks connected in cascade are defined (T_A, T_B and T_N), the property of the wave cascade matrix can be applied in order to compute the error coefficients of T_A and T_B by connecting and measuring the standards.

Since the error coefficients have to be determined, a Thru (L_1) and a Line (L_2) standards which are non-reflective lines have to be used in the TRL calibration technique. In one hand, a Thru standard has to be connected, that is, a direct connection of the VNA cables placing a reference plane at the end of them, in case that this is not possible, the smallest line of the calibration standards has to be connected, this small line acts as a Thru, moving the reference plane (Fig. 2.4). On the other hand a Line standard is connected with the constrain $L_1 < L_2$ (See Fig. 2.5).

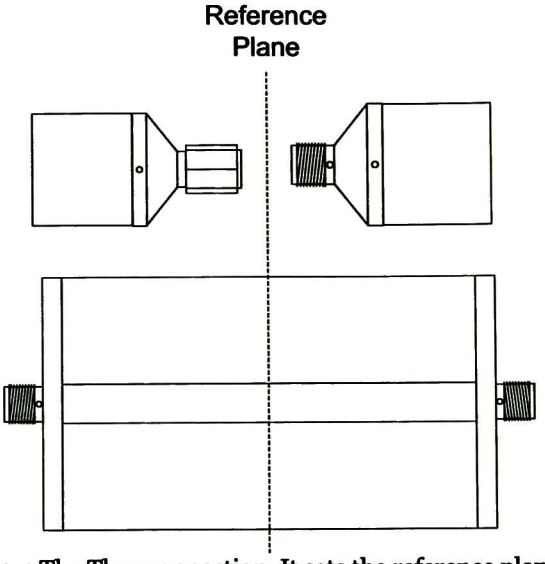

Fig. 2.4 The Thru connection. It sets the reference plane.

The measured S parameters of the Thru standard is converted to T T_{LREF} parameters and represented as eq. (2.19) where T_N is substituted by the T parameters of the Thru

$$T_{LREF} = T_A T_{L1} T_B \qquad (2.23)$$

for the line standard:

$$T_2 = T_A T_{L2} T_B \qquad (2.24)$$

where

- T_{LREF} are the T-parameters measured of L_1 (Thru) connected to the ports.
- T_2 are the T-parameters measured of L_2 connected to the ports.
- T_A and T_B are the error boxes T-parameters.

It is important to recall that T_A and T_B have the VNA systematic errors, including the transition errors (i.e.: Microstrip-coaxial, connectors).

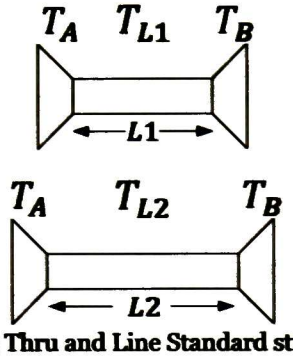

Fig. 2.5 Thru and Line Standard structure

Also, the T parameters of any non-reflective line (T_{LN}) is defined as

$$T_L = \begin{bmatrix} e^{-\gamma L} & 0 \\ 0 & e^{\gamma L} \end{bmatrix} \quad (2.25)$$

For simplicity, from (2.23) and (2.24) T_B can be eliminated from the computations and allows us to know partially the error coefficients of T_A (a/c and b) and also the propagation constant γ. Hence:

$$T = T_2 T_{LREF}^{-1} = T_A T_{L2} T_{L1}^{-1} T_A^{-1} \quad (2.26)$$

Where T_{L1} and T_{L2} are defined according to the model of eq. (2.25). The product of these matrices is

$$T_\Psi = T_{L2} T_{L1}^{-1} = \begin{bmatrix} e^{-\gamma L_T} & 0 \\ 0 & e^{\gamma L_T} \end{bmatrix} \quad (2.27)$$

where

$$L_T = L_2 - L_1 \quad (2.28)$$

redefining eq. (2.26)

$$T = T_A T_\Psi T_A^{-1} \quad (2.29)$$

from the equation (2.27) it can be seen that T_Ψ has the following form

$$T_\Psi = \begin{bmatrix} 1/\Psi & 0 \\ 0 & \Psi \end{bmatrix} \quad (2.30)$$

where

$$\Psi = e^{\gamma L_T}$$

Matrices T_1 and T_2 are known matrices obtained from VNA measurements. For simplicity T matrix can be represented as follows

$$T = T_2 T_1^{-1} = \begin{bmatrix} t_{11} & t_{12} \\ t_{21} & t_{22} \end{bmatrix} \quad (2.31)$$

From (2.29) it can be observed that T and T_Ψ are similar matrices. Solving for T_Ψ, the following equation is obtained

$$T_\Psi = T_A^{-1} T T_A \quad (2.32)$$

Substituting the symbols by the defined matrices mentioned above having

$$\begin{bmatrix} 1/\Psi & 0 \\ 0 & \Psi \end{bmatrix} = \left(\frac{1}{a - bc}\right) \begin{bmatrix} 1 & -b \\ -c & a \end{bmatrix} \begin{bmatrix} t_{11} & t_{12} \\ t_{21} & t_{22} \end{bmatrix} \begin{bmatrix} a & b \\ c & 1 \end{bmatrix} \quad (2.33)$$

solving the matrices product the following matrix is obtained

$$T_\Psi = \begin{bmatrix} T_{\Psi 11} & T_{\Psi 12} \\ T_{\Psi 21} & T_{\Psi 22} \end{bmatrix}$$

$$T_\Psi = q \begin{bmatrix} at_{11} + ct_{12} - abt_{21} - bct_{22} & b^2 t_{21} + b(t_{22} - t_{11}) - t_{12} \\ \left(\frac{a}{c}\right)^2 t_{21} + \left(\frac{a}{c}\right)(t_{22} - t_{11}) - t_{12} & -bct_{11} - ct_{12} + abt_{21} + at_{22} \end{bmatrix} \quad (2.34)$$

where

$$q = \frac{1}{(a - bc)}$$

According to (2.33) and (2.34), $T_{\Psi 12}$ and $T_{\Psi 21}$ are equal to zero

$$b^2 t_{21} + b(t_{22} - t_{11}) - t_{12} = 0 \quad (2.35)$$

$$\left(\frac{a}{c}\right)^2 t_{21} + \left(\frac{a}{c}\right)(t_{22} - t_{11}) - t_{12} = 0 \quad (2.36)$$

It is seen that the polynomials shown in (2.35) and (2.36) have the same coefficients and so a/c and b are roots of the same equation. It is known that if T_A is invertible its determinant must be different from zero

$$\det(T_A) = a - bc \neq 0$$

therefore

$$\frac{a}{c} \neq b$$

This means the polynomials used to determine a/c and b are the same, in consequence, the roots obtained are equal. By solving the polynomial, b will be one of the roots obtained and a/c will be the other root obtained. Engen and Hoer [2] say that the ratio of the absolute values of the two roots $|b|/|a/c|$ will lead to the following unequality

$$|b| < \left|\frac{a}{c}\right|$$

Furthermore, the wave propagation vector Ψ can be obtained directly from eq. (2.34)

$$\Psi = \frac{t_{22} + bt_{21} - \frac{b}{a/c}t_{11} - \frac{1}{a/c}t_{12}}{1 - \left(\frac{b}{a/c}\right)} = \frac{1 - \left(\frac{b}{a/c}\right)}{t_{11} + \frac{b}{a/c}t_{12} - bt_{21} - \frac{b}{a/c}t_{12}} \qquad (2.37)$$

Once Ψ is computed, the electrical length from the lines can be determined by

$$\Delta\phi = \tan^{-1}\left[\frac{Im(\Psi)}{Re(\Psi)}\right] \qquad (2.38)$$

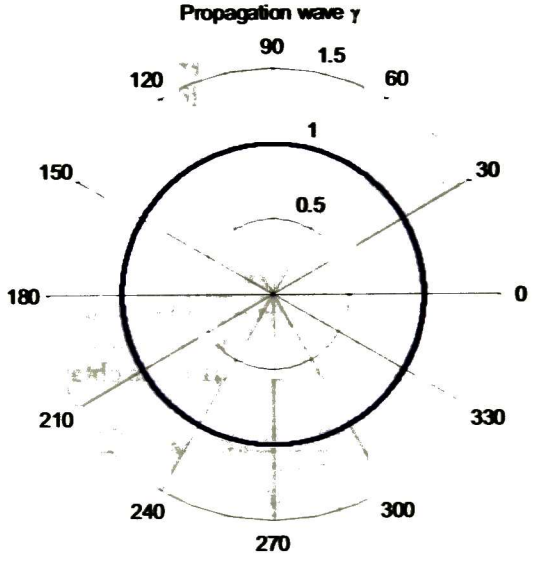

Fig. 2.6 Polar plot of the propagation wave behavior.

knowing Ψ, the wave propagation constant can be obtained as follows

$$\gamma = \frac{\ln(\Psi)}{l_2 - l_1}$$

where

$$\gamma = \alpha + j\beta$$

It should be noticed, that for the wave propagation constant computation, the length of the lines have to be known.

So far, the known values a/c and b, are partial values from the error box A, where the L_{REF} and L_2 were used for its computation.

In order to find the coefficients within the matrix of the error box A and separate the values a and c, the reference line is used, noticing that, there is a dependence on error box B.

The measured wave cascade matrix of the reference line, was defined in (2.23) and in general, it can be represented as

$$T_L = g\begin{bmatrix} d & e \\ f & 1 \end{bmatrix} \tag{2.39}$$

from (2.23) T_B is found to be

$$T_B = T_{LREF}^{-1} T_A^{-1} T_L \tag{2.40}$$

Thus far, the measured transmission line T_L is the wave cascade matrix of the line used in the TRL calibration modeled in (2.39). Which is the error box A T_A, cascaded with the ideal line T_{LREF} and the error box B T_B. The error box A T_A is partially known (a/c and b), the measured line T_L and the model of the ideal line T_{LREF} are be completely known.

Now, substituting (2.20), (2.22), (2.25) and (2.39) into (2.40) the product is represented as

$$\rho_{22}\begin{bmatrix} \alpha & \beta \\ \varphi & 1 \end{bmatrix} = \begin{bmatrix} e^{\gamma L_{LREF}} & 0 \\ 0 & e^{-\gamma L_{LREF}} \end{bmatrix} \frac{1}{\tau_{22}(a - bc)} \begin{bmatrix} 1 & -b \\ -c & a \end{bmatrix} g \begin{bmatrix} d & e \\ f & 1 \end{bmatrix} \tag{2.41}$$

Developing the product and simplifying (2.41), it is obtained

$$\rho_{22}\begin{bmatrix} \alpha & \beta \\ \varphi & 1 \end{bmatrix} = \frac{g(a - ce)e^{-\gamma L_{LREF}}}{\tau_{22}(a - bc)} \begin{bmatrix} \frac{d - bf}{a - ce} e^{2\gamma L_{LREF}} & \frac{e - b}{a - ce} e^{2\gamma L_{LREF}} \\ \frac{af - cd}{a - ce} & 1 \end{bmatrix} \tag{2.42}$$

The terms of both sides of (2.42) are compared term by term

$$\alpha = \frac{d - bf}{a - ce} e^{2\gamma L_{LREF}} \tag{2.43}$$

$$\beta = \frac{e - b}{a - ce} e^{2\gamma L_{LREF}} \tag{2.44}$$

$$\varphi = \frac{\frac{a}{c} f - d}{\frac{a}{c} - e} \tag{2.45}$$

$$\rho_{22}\tau_{22} = \frac{g(a - ce)}{(a - bc)} e^{-\gamma L_{LREF}} \tag{2.46}$$

Taking the ratio of β and α will provide a result that is not dependent on the propagation constant (γ) nor the length of the reference line

$$\frac{\beta}{\alpha} = \frac{e-b}{d-bf} \tag{2.47}$$

Eq. (2.43) is rearranged in terms of a/c

$$\alpha a = \frac{d-bf}{1-\frac{c}{a}e} e^{2\gamma L_{LREF}} \tag{2.48}$$

Up to this point, the remaining error terms cannot be computed unless a or c are determined. In that sense, a reflect standard with or without an offset is connected so that the value of a is found.

Thus, connecting a reflect (a short or an open) at each port, the one port error model, explained in section 1.6.1, is applied and solved in order to obtain a measured Γ_{meas} for each port in terms of the real Γ_R.

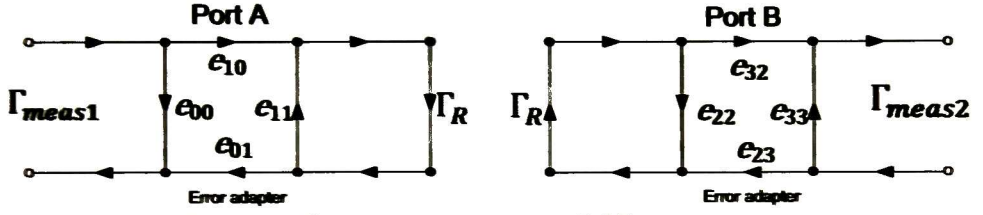

Fig. 2.7 Reflect measurement model for two ports.

From the one port error model, the solution of the flow graph of the model of port A (Fig. 2.7) is

$$\Gamma_{meas1} = \frac{e_{00} + \Gamma_r(e_{10}e_{01} - e_{00}e_{11})}{1 - e_{11}\Gamma_R} \tag{2.49}$$

$$\Gamma_{meas1} = \frac{a\Gamma_R + b}{c\Gamma_R + 1} \tag{2.50}$$

and for port B is

$$\Gamma_{meas2} = \frac{e_{33} + \Gamma_R(e_{32}e_{23} - e_{22}e_{33})}{1 - e_{22}\Gamma_R} \tag{2.51}$$

$$\Gamma_{meas2} = \frac{a\Gamma_R - \varphi}{1 - \beta\Gamma_R} \tag{2.52}$$

Solving both ports for the real reflection coefficient Γ_R it is obtained

$$\Gamma_R = \frac{b - \Gamma_{meas1}}{c\Gamma_{meas1} - a} \tag{2.53}$$

$$\Gamma_R = \frac{\varphi + \Gamma_{meas2}}{\alpha + \beta\Gamma_{meas2}} \quad (2.54)$$

Assuming that the real reflection coefficient at each port is the same, and equating (2.53) and (2.54), the ratio a/α as a function of c/a and β/α, can be computed

$$\frac{b - \Gamma_{meas1}}{c\Gamma_{meas1} - a} = \frac{\varphi + \Gamma_{meas2}}{\alpha + \beta\Gamma_{meas2}} \quad (2.55)$$

$$\frac{a}{\alpha} = \frac{(b - \Gamma_{meas1})\left(1 + \frac{\beta}{\alpha}\Gamma_{meas2}\right)}{\left(\frac{c}{a}\Gamma_{meas1} - 1\right)(\varphi + \Gamma_{meas2})} \quad (2.56)$$

Substituting (2.48) into (2.56), an analytical expression for a can now be found as:

$$a = \pm\sqrt{\frac{(d - bf)(b - \Gamma_{meas1})\left(1 + \frac{\beta}{\alpha}\Gamma_{meas2}\right)}{\left(1 - \frac{c}{a}e\right)(\varphi + \Gamma_{meas2})\left(\frac{c}{a}\Gamma_{meas1} - 1\right)}}e^{\gamma L_{line}} \quad (2.57)$$

According to (2.57), it is seen that two roots are found, with the same magnitude but with different sign. Selecting the incorrect root will lead to miscalculations in the calibration process. Thus, to distinguish the correct root, an estimate a ($\hat{a}$) should be computed from (2.53), in which the reflect is assumed without offset ($\Gamma_r = -1$ for a short and $\Gamma_r = 1$ for an open), this is a necessary and sufficient condition

$$\hat{a} = \frac{b - \Gamma_{meas1}}{\Gamma_R(\frac{c}{a}\Gamma_{meas1} - 1)} \quad (2.58)$$

Since the objective is to determine the sign of a, an error function is defined

$$err = |\pm a - \hat{a}| \quad (2.59)$$

where the minimum error will determine the correct sign for a of eq. (2.57), in consequence, the c term in the error box A can be evaluated from the maximum absolute value of the roots in (2.36).

Notice that once a is computed, the terms α, β and φ can be evaluated from (2.43)-(2.45). Finally the product $\rho_{22}r_{22}$ from (2.46) is used to de-embed the real S parameter of a DUT.

2.2.3 Line-Reflect-Reflect-Match (LRRM) Calibration Technique

This technique computes the VNA systematic errors by using four standards (Fig. 2.8): Line, Open, Short and a Match. Most of the error coefficients are determined by the one port error model, this is the key of this technique. The

use of a match standard makes easy to find the error coefficients b and φ, from error box T_A and T_B respectively.

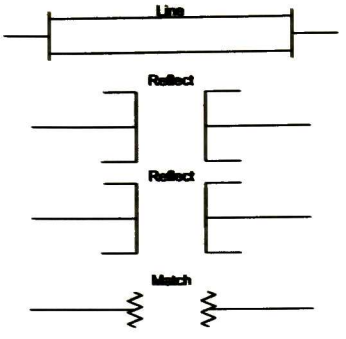

Fig. 2.8 Line, Reflect, Reflect, Match standards

The measurement of two Reflect standards; an Open and a Short is the central point of this calibration. From the previous experience of the TRL calibration technique, it is known that a and c cannot be found directly, rather, a/c ratio is computed first. This is why the following procedure will be applied.

For the reflect standards, the one port error model is utilized (Fig. 2.7). Measuring the reflection coefficient for the first reflect (open or short) used at both ports it is obtained

$$w_1 = \frac{b + a\Gamma_{R1}}{1 + c\Gamma_{R1}} \tag{2.60}$$

$$w_2 = \frac{a\Gamma_{R1} - \varphi}{1 - \beta\Gamma_{R1}} \tag{2.61}$$

The reflection coefficients of the second reflect (if an open was used on the first reflect a short must be used and conversely) measured at both ports are

$$\mu_1 = \frac{b + a\,\Gamma_{R2}}{1 + c\Gamma_{R2}} \tag{2.62}$$

$$\mu_2 = \frac{a\Gamma_{R2} - \varphi}{1 - \beta\Gamma_{R2}} \tag{2.63}$$

Solving for Γ_{R1} at both equations (2.60) and (2.61), it is obtained

$$\Gamma_{R1} = \frac{b - w_1}{cw_1 - a} \tag{2.64}$$

$$\Gamma_{R1} = \frac{w_2 + \varphi}{a + \beta w_2} \tag{2.65}$$

and with Γ_{R2} (2.62)and (2.63)

$$\Gamma_{R2} = \frac{b - \mu_1}{c\mu_1 - a} \tag{2.66}$$

$$\Gamma_{R2} = \frac{\mu_2 + \varphi}{\alpha + \beta\mu_2} \tag{2.67}$$

Equating Γ_{R1} in (2.64) and (2.65), it is obtained

$$\frac{a\alpha(b - w_1)}{\frac{c}{a}w_1 - 1} = \frac{a^2(w_2 + \varphi)}{1 + \frac{\beta}{\alpha}w_2} \tag{2.68}$$

Equating Γ_{R2} in (2.66) and (2.67)

$$\frac{a\alpha(b - \mu_1)}{\frac{c}{a}\mu_1 - 1} = \frac{a^2(\mu_2 + \varphi)}{1 + \frac{\beta}{\alpha}\mu_2} \tag{2.69}$$

Expanding eq. (2.68) and (2.69)

$$a\alpha(b - w_1)\left(1 + \frac{\beta}{\alpha}w_2\right) = a^2(w_2 + \varphi)\left(\frac{c}{a}w_1 - 1\right) \tag{2.70}$$

$$a\alpha(b - \mu_1)\left(1 + \frac{\beta}{\alpha}\mu_2\right) = a^2(\mu_2 + \varphi)\left(\frac{c}{a}\mu_1 - 1\right) \tag{2.71}$$

By taking the ratio of (2.70), (2.71) and simplifying, eq. (2.72) is obtained

$$\frac{(b - w_1)\left(1 + \frac{\beta}{\alpha}w_2\right)}{(b - \mu_1)\left(1 + \frac{\beta}{\alpha}\mu_2\right)} = \frac{(w_2 + \varphi)\left(\frac{c}{a}w_1 - 1\right)}{(\mu_2 + \varphi)\left(\frac{c}{a}\mu_1 - 1\right)} \tag{2.72}$$

defining

$$(b - w_1)\left(1 + \frac{\beta}{\alpha}w_2\right) = x \tag{2.73}$$

$$(b - \mu_1)\left(1 + \frac{\beta}{\alpha}\mu_2\right) = y \tag{2.74}$$

Substituting (2.73) and (2.74) into (2.72)

$$x(\mu_2 + \varphi)\left(\frac{c}{a}\mu_1 - 1\right) = (w_2 + \varphi)\left(\frac{c}{a}w_1 - 1\right)y \tag{2.75}$$

the binomial products are performed and rearranging terms

$$\frac{c}{a}\left(\frac{x}{y}\mu_1\mu_2 - w_1w_2\right) + \frac{c}{a}\varphi\left(\frac{x}{y}\mu_1 - w_1\right) - \varphi\left(\frac{x}{y} - 1\right) - \left(\frac{x}{y}\mu_2 - w_2\right) = 0 \tag{2.76}$$

Eq. (2.76) can be rewritten as

$$\frac{c}{a}k_1 + \frac{c}{a}\varphi k_2 - \varphi k_3 - k_4 = 0 \qquad (2.77)$$

where

$$k_1 = \frac{x}{y}\mu_1\mu_2 - w_1w_2 \qquad (2.78)$$

$$k_2 = \frac{x}{y}\mu_1 - w_1 \qquad (2.79)$$

$$k_3 = \frac{x}{y} - 1 \qquad (2.80)$$

$$k_4 = \frac{x}{y}\mu_2 - w_2 \qquad (2.81)$$

To this point, it is seen, that the reflection coefficient in (2.67) still depends on β/α. This relation is found with the Thru standard measurement. In addition, $\alpha, \beta, \varphi, \rho_{22}$ are also computed in terms of c/a and b.

In this calibration technique the Thru is a non-reflective transmission line, this implies, that the wave propagation constant γ has to be known and there is no direct procedure without the use of another transmission line. Thus, for convenience, the reference plane is set at the middle of the Thru (i.e.: $L_{REF} = 0$).

Recalling from TRL calibration (section 2.2.2) eq. (2.39) to (2.46), and based on the condition stated above, the error coefficients of the error box B (T_B) are

$$\alpha = \frac{d - bf}{a - ce} \qquad (2.82)$$

$$\beta = \frac{e - b}{a - ce} \qquad (2.83)$$

$$\varphi = \frac{f - \frac{c}{a}d}{1 - \frac{c}{a}e} \qquad (2.84)$$

$$\rho_{22}r_{22} = \frac{g(a - ce)}{(a - bc)} \qquad (2.85)$$

hence

$$\frac{\beta}{\alpha} = \frac{e - b}{d - bf} \qquad (2.86)$$

a quadratic equation in terms of c/a can be found by substituting (2.84) into (2.77)

$$\left(\frac{c}{a}\right)^2 (k_1 e + dk_2) - \frac{c}{a}(k_1 + fk_2 + dk_3 + ek_4) + (fk_3 + k_4) = 0 \qquad (2.87)$$

The only unknown value of equation (2.87) is φ, which can be found with the match. It is known that, when a match is measured the only value obtained in equation (2.60) and (2.63) is φ.

Again the roots selection problem is found as in the TRL calibration technique. To overcome this problem, c/a has to satisfy the following inequality

$$\left|\frac{c}{a}\right| < \left|\frac{1}{b}\right|$$

The value of a has to be chosen in the same way as in the TRL calibration. A reflect measurement (either the Open or Short), along with the Thru measurement (2.57), where the problem of sign will be again present. The estimated value $\hat{a}$ in (2.58) will provide the actual value of a by the error function defined in (2.59). Finally the error box B (T_B) can be computed from (2.82)-(2.85).

Chapter 3

De-Embedding

Once the VNA systematic errors have been estimated, a procedure is needed to displace the measurement reference plane from the ideal VNA to the DUT. From the VNA diagram explained on earlier chapters, the ideal VNA is followed by error boxes A and B and between these error boxes is the DUT. Hence the measurement has to be moved from the ideal VNA through the DUT, this process is called de-embedding.

This chapter covers two de-embedding methodologies that help obtaining the actual S parameters of a DUT: the classic method and the straigh-forward Method. The Classic method evaluates all the error boxes parameters while the Straight-forward method saves computation of an error box assuming symmetry.

3.1 VNA model

From the VNA model explained in Fig. 2.2, the error boxes A and B are cascaded with the DUT. The measurements received come with the systematic errors, and the latter have already been estimated in Chapter 2.

In this chapter, a procedure to de-embed the measurement in order to obtain the actual S parameters of the DUT will be developed.

The model for the eight error term [13] developed by Hackborn will be presented in this work, where the Error Box A and the Transition Errors as one

box and the Error Box B and the Transition Errors as another box is computed. These boxes are represented as T_A and T_B respectively.

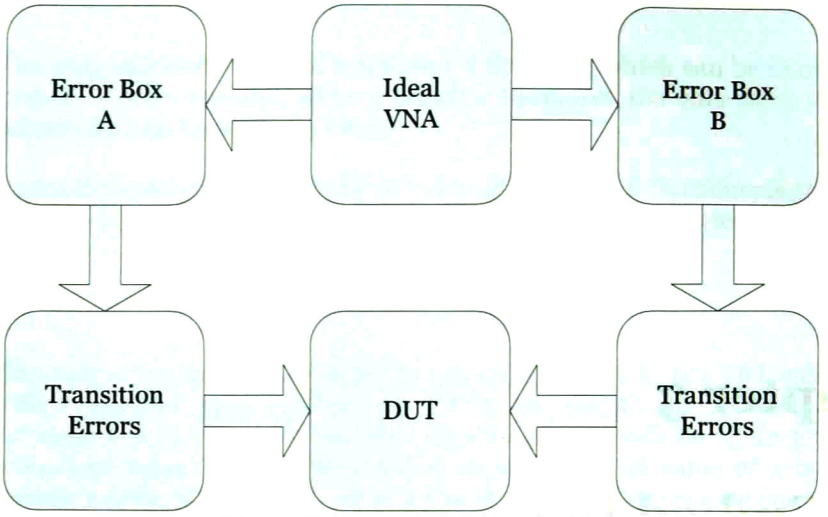

Fig. 3.1 VNA and the DUT connection model

The error boxes T_A and T_B are modeled as

$$T_A = r_{22}\begin{bmatrix} a & b \\ c & 1 \end{bmatrix} \quad (3.1)$$

$$T_B = \rho_{22}\begin{bmatrix} \alpha & \beta \\ \varphi & 1 \end{bmatrix} \quad (3.2)$$

There are times when the DUT will be inside transmission lines, in this case, knowing the model will be important to de-embed and so, obtain the actual S parameters of the DUT.

The transmission parameters (T_{Lx}) matrix of a uniform transmission line with length L_x (where $x \epsilon \mathbb{R} \wedge x > 0$), arbitrary impedance and an unknown Z_L is represented by

$$T_{Lx} = \frac{1}{(1-\Gamma^2)e^{-\gamma Lx}}\begin{bmatrix} e^{-2\gamma Lx} - \Gamma^2 & \Gamma(1-e^{-2\gamma Lx}) \\ -\Gamma(1-e^{-2\gamma Lx}) & 1-\Gamma^2 e^{-2\gamma Lx} \end{bmatrix} \quad (3.3)$$

Reynoso-Hernández [15] states that the above equation can be rewritten as follows:

$$T_{Lx} = \begin{bmatrix} 1 & \Gamma \\ \Gamma & 1 \end{bmatrix}\begin{bmatrix} e^{-\gamma Lx} & 0 \\ 0 & 1/e^{-\gamma Lx} \end{bmatrix}\frac{1}{(1-\Gamma^2)}\begin{bmatrix} 1 & -\Gamma \\ -\Gamma & 1 \end{bmatrix} \quad (3.4)$$

Where γ is the propagation constant; this equation allows determining the reflection coefficient Γ and the propagation vector $e^{-\gamma Lx}$.
For the TRL calibration technique this model is used assuming that the transmission lines are non-reflective (i.e.: $\Gamma = 0$), resulting in the following.

$$T_{Lx} = \begin{bmatrix} e^{-\gamma L_x} & 0 \\ 0 & e^{\gamma L_x} \end{bmatrix} \quad (3.5)$$

3.3 Classic Method

Once the calibration has been made, that is, the error boxes A and B have been estimated, the systematic errors have to be eliminated from the measurement and the corrected S parameters can now be obtained, the de-embedding process is in charge of it.

Recalling the VNA model connected with a DUT in Fig. 2.2. The cascaded connection of the VNA with a DUT is now modeled in cascade wave matrix from:

$$T_{MDUT} = T_A T_{DUT} T_B \quad (3.6)$$

where

- T_{MDUT} is the measured T parameters of the DUT from the VNA with all the implicated connections represented as

$$T_{MDUT} = \begin{bmatrix} m_{11} & m_{12} \\ m_{21} & m_{22} \end{bmatrix} \quad (3.7)$$

- T_A is the transmission matrix of the transition at the port 1.
- T_B is the transmission matrix of the transition at the port 2.
- T_{DUT} is the transmission matrix of the actual parameters of the DUT.

The main goal of the de-embedding process is to find the actual S parameters of the DUT. Thus, eq. 3.6 has to be solved for T_{DUT}.

$$T_{DUT} = T_A^{-1} T_{MDUT} T_B^{-1} \quad (3.8)$$

Recalling that:

$$T_A = r_{22} \begin{bmatrix} a & b \\ c & 1 \end{bmatrix} \quad (3.9)$$

$$T_B = \rho_{22} \begin{bmatrix} \alpha & \beta \\ \varphi & 1 \end{bmatrix} \quad (3.10)$$

Then, substituting the models (3.9) and (3.10) into (3.8) it is obtained

$$T_{DUT} = k \begin{bmatrix} t_{11} & t_{12} \\ t_{21} & t_{22} \end{bmatrix} \quad (3.11)$$

where

$$t_{11} = m_{11} - b m_{21} - \varphi m_{12} + b\varphi m_{22}$$

$$t_{12} = -\beta m_{11} + b\beta m_{21} + \alpha m_{12} - b\alpha m_{22}$$

$$t_{21} = -cm_{11} + am_{21} + c\varphi m_{12} - a\varphi m_{22}$$

$$t_{22} = c\beta m_{11} - a\beta m_{21} - c\alpha m_{12} + a\alpha m_{22}$$

$$k = \frac{1}{r_{22}\rho_{22}(a - bc)(\alpha - \beta\varphi)}$$

Recalling the transformation from S parameters to wave cascade matrix (2.18), it can be easily shown that the S parameters are

$$S_{21} = \frac{1}{kt_{22}} \qquad (3.12)$$

$$S_{11} = \frac{t_{12}}{t_{22}} \qquad (3.13)$$

$$S_{22} = -\frac{t_{21}}{t_{22}} \qquad (3.14)$$

$$S_{12} = k\left(t_{11} - \frac{t_{12}t_{21}}{t_{22}}\right) \qquad (3.15)$$

Notice the dependence on a, b, c, α, β and φ.

3.4 Straight-Forward Method

The Straight-forward method combines the measurement of a Thru standard (the reference line L_{REF}), with the DUT measurement [16], to avoid the complete evaluation of the error box B (i.e.: T_B). It should be noted that, the Thru must be completely known.

Since the measurements are represented in cascade wave form, the Thru measurement is

$$T_1 = T_A T_{LREF} T_B \qquad (3.16)$$

where

- T_1 is the T-parameter matrix for the reference line measured data coming from the VNA.
- T_A is the T-parameter matrix for the error box A
- T_B is the T-parameter matrix for the error box B
- T_{LREF} is the T-parameter matrix for the reference line of the actual parameters with length T_{LREF}.

And let it be

$$T_2 = T_A T_D T_B \qquad (3.17)$$

where

- T_2 is the T-parameter matrix of the DUT between the two transmission lines with length L and the error boxes A and B.
- T_D is the T-parameter matrix of the DUT.

By solving (3.17) and (3.16) for T_D and T_{LREF} respectively it can be written as the following product:

$$T_D T_{LREF}^{-1} = T_A^{-1} T_2 T_1^{-1} T_A = \frac{1}{(a-bc)} \begin{bmatrix} N_{11} & N_{12} \\ N_{21} & N_{22} \end{bmatrix} \quad (3.18)$$

as T_1 and T_2 are known matrices, a new matrix is defined as

$$P = T_2 T_1^{-1} = \begin{bmatrix} p_{11} & p_{12} \\ p_{21} & p_{22} \end{bmatrix} \quad (3.19)$$

hence

$$N_{11} = a\left(p_{11} + \frac{c}{a} p_{12} - b p_{21} - b\frac{c}{a} p_{22}\right) \quad (3.20)$$

$$N_{12} = b p_{11} + p_{12} - b^2 p_{21} - b p_{22} \quad (3.21)$$

$$N_{21} = a^2\left[-\frac{c}{a} p_{11} - \left(\frac{c}{a}\right)^2 p_{12} + p_{21} + \frac{c}{a} p_{22}\right] \quad (3.22)$$

$$N_{22} = a\left(-b\frac{c}{a} p_{11} - \frac{c}{a} p_{12} + b p_{21} + p_{22}\right) \quad (3.23)$$

notice from (3.18) that the computation of error box B is no longer needed.

If the left term of (3.18) is converted to S parameters, it is obtained

$$\frac{1}{S_{21}} \begin{bmatrix} -\Delta S e^{-\gamma L_{REF}} & S_{11} e^{-\gamma L_{REF}} \\ -S_{22} e^{\gamma L_{REF}} & e^{\gamma L_{REF}} \end{bmatrix} = \frac{1}{(a-bc)} \begin{bmatrix} N_{11} & N_{12} \\ N_{21} & N_{22} \end{bmatrix} \quad (3.24)$$

where all S parameters except S_{12} can easily be evaluated.

Noting that $T_D T_{LREF}^{-1}$ and $T_2 T_1^{-1}$ are similar matrices and therefore their determinant are the same (See Appendix A). S_{12} can be easily found, by taking the determinant of $T_2 T_1^{-1}$ on equation (3.19) and equation (3.24) obtaining

$$(p_{11} p_{22} - p_{12} p_{21}) = \frac{S_{12}}{S_{21}} \quad (3.25)$$

from the above result it is assumed that S_{21} has been already computed obtaining the following S-parameters.

$$S_{11} = \frac{-\frac{a}{c}[b^2 p_{21} + b(p_{22} - p_{11}) - p_{12}]}{a_f\left[\frac{a}{c}p_{22} + b\left(\frac{a}{c}p_{21} - p_{11}\right) - p_{12}\right]} e^{\gamma(L_{REF})} \qquad (3.26)$$

$$S_{12} = \Delta p \frac{\left(\frac{a}{c} - b\right)}{\frac{a}{c}p_{22} + b\left(\frac{a}{c}p_{21} - p_{11}\right) - p_{12}} e^{\gamma(L_{REF})} \qquad (3.27)$$

$$S_{21} = \frac{\left(\frac{a}{c} - b\right)}{\left[\frac{a}{c}p_{22} + b\left(\frac{a}{c}p_{21} - p_{11}\right) - p_{12}\right]} e^{\gamma(L_{REF})} \qquad (3.28)$$

$$S_{22} = \frac{-\left[\left(\frac{a}{c}\right)^2 p_{21} + \frac{a}{c}(p_{22} - p_{11}) - p_{12}\right]}{\frac{a}{c}\left[\frac{a}{c}p_{22} + b\left(\frac{a}{c}p_{21} - p_{11}\right) - p_{12}\right]} a_f e^{\gamma(L_{REF})} \qquad (3.29)$$

where

$$a_f = a e^{-\gamma L_{REF}}$$

equations (3.26)-(3.29) are generic for the straight-forward de-embedding, because they allow the computing of the S Parameters of the DUT with the complete knowledge of the error box A and a partial knowledge of the error box B.

Depending on the device connection equations (3.26)-(3.29) can be adjusted depending where the reference plane is set. There are three possible cases:

a) When the reference plane and the DUT is set at the middle of the Thru, $L_{REF} = L = 0$
b) When the DUT is between Transmission lines two times greater than the Thru, $L_{REF} = 2L$
c) When the DUT is connected right after the transition, $L_{REF} \neq 0;\ L = 0$

where L is a line contained in the DUT, converting the T parameter matrix of the DUT to $T_D = T_L T_{DUT} T_L$.

The case a) can be applied to coaxial devices where the reference line L_{REF} and the line lengths L inserted in the test fixture are zero (i.e.: $L_{REF} = L = 0$). These equations are simplified avoiding the propagation constant computation and a_f is simplified to just a.

$$S_{11} = \frac{-\frac{a}{c}[b^2 p_{21} + b(p_{22} - p_{11}) - p_{12}]}{a_f\left[\frac{a}{c}p_{22} + b\left(\frac{a}{c}p_{21} - p_{11}\right) - p_{12}\right]} \qquad (3.30)$$

$$S_{12} = \Delta p \frac{\left(\frac{a}{c} - b\right)}{\frac{a}{c}p_{22} + b\left(\frac{a}{c}p_{21} - p_{11}\right) - p_{12}} \quad (3.31)$$

$$S_{21} = \frac{\left(\frac{a}{c} - b\right)}{\left[\frac{a}{c}p_{22} + b\left(\frac{a}{c}p_{21} - p_{11}\right) - p_{12}\right]} \quad (3.32)$$

$$S_{22} = \frac{-\left[\left(\frac{a}{c}\right)^2 p_{21} + \frac{a}{c}(p_{22} - p_{11}) - p_{12}\right]}{\frac{a}{c}\left[\frac{a}{c}p_{22} + b\left(\frac{a}{c}p_{21} - p_{11}\right) - p_{12}\right]} a \quad (3.33)$$

The case b) can be applied for devices mounted over test fixtures where the total length of the lines that connects the DUT are equal to the reference line (i.e.: $L_{REF} = 2L$). This simplifies the equations (3.26)-(3.29) but still leaves the propagation constant to compute as $a_f = e^{-\gamma L_{REF}}$:

$$S_{11} = \frac{-\frac{a}{c}[b^2 p_{21} + b(p_{22} - p_{11}) - p_{12}]}{a_f\left[\frac{a}{c}p_{22} + b\left(\frac{a}{c}p_{21} - p_{11}\right) - p_{12}\right]} \quad (3.34)$$

$$S_{12} = \Delta p \frac{\left(\frac{a}{c} - b\right)}{\frac{a}{c}p_{22} + b\left(\frac{a}{c}p_{21} - p_{11}\right) - p_{12}} \quad (3.35)$$

$$S_{21} = \frac{\left(\frac{a}{c} - b\right)}{\left[\frac{a}{c}p_{22} + b\left(\frac{a}{c}p_{21} - p_{11}\right) - p_{12}\right]} \quad (3.36)$$

$$S_{22} = \frac{-\left[\left(\frac{a}{c}\right)^2 p_{21} + \frac{a}{c}(p_{22} - p_{11}) - p_{12}\right]}{\frac{a}{c}\left[\frac{a}{c}p_{22} + b\left(\frac{a}{c}p_{21} - p_{11}\right) - p_{12}\right]} a_f \quad (3.37)$$

The case c) can be applied for wafer devices (when the calibration is at the end of the probes) $L_{REF} \neq 0$; $L = 0$. When the DUT is in direct contact to the probes, the line where the DUT is located is zero (i.e.: $L = 0$). Commercially the standards are found to be with a line of short length for the Thru and it is the one used as reference.

$$S_{11} = \frac{-\frac{a}{c}[b^2 p_{21} + b(p_{22} - p_{11}) - p_{12}]}{a_f\left[\frac{a}{c}p_{22} + b\left(\frac{a}{c}p_{21} - p_{11}\right) - p_{12}\right]} e^{\gamma(L_{REF})} \quad (3.38)$$

$$S_{12} = \Delta p \frac{\left(\frac{a}{c} - b\right)}{\frac{a}{c}p_{22} + b\left(\frac{a}{c}p_{21} - p_{11}\right) - p_{12}} e^{\gamma(L_{REF})} \quad (3.39)$$

$$S_{21} = \frac{\left(\frac{a}{c} - b\right)}{\left[\frac{a}{c}p_{22} + b\left(\frac{a}{c}p_{21} - p_{11}\right) - p_{12}\right]} e^{\gamma(L_{REF})} \quad (3.40)$$

$$S_{22} = \frac{-\left[\left(\frac{a}{c}\right)^2 p_{21} + \frac{a}{c}(p_{22} - p_{11}) - p_{12}\right]}{\frac{a}{c}\left[\frac{a}{c}p_{22} + b\left(\frac{a}{c}p_{21} - p_{11}\right) - p_{12}\right]} a_f e^{\gamma(L_{REF})} \quad (3.41)$$

3.5 $e^{\gamma L}$ Computation

There is a problem when solving eq. (3.26)-(3.29) when the connection to the device is not coaxial (in fixture and on wafer). This problem is the computation of a_f. The computation is performed by using a symmetric reflector element at port A and port B where their reflection coefficients Γ_{R1} and Γ_{R2} are unknown. The measured reflection coefficients Γ_{M1} and Γ_{M2} can be represented as a function of Γ_{R1} and Γ_{R2} as follows

$$\Gamma_{M1} = \frac{a\Gamma_{R1} + b}{c\Gamma_{R1} + 1} \quad (3.42)$$

$$\Gamma_{M2} = \frac{\alpha\Gamma_{R2} - \varphi}{1 - \beta\Gamma_{R2}} \quad (3.43)$$

Knowing that a symmetrical reflector element is used, the reflection coefficients are equal (i.e.: $\Gamma_{R1} = \Gamma_{R2}$), hence

$$\frac{\Gamma_{M1} - b}{a\left(1 - \frac{c}{a}\Gamma_{M1}\right)} = \frac{\Gamma_{M2} + \varphi}{\alpha\left(1 + \frac{\beta}{\alpha}\Gamma_{M2}\right)} \quad (3.44)$$

Solving for a/α it is obtained

$$\frac{a}{\alpha} = \frac{(\Gamma_{M1} - b)\left(1 + \frac{\beta}{\alpha}\Gamma_{M2}\right)}{\left(1 + \frac{c}{a}\right)(\Gamma_{M2} + \varphi)} \quad (3.45)$$

a cannot be computed if α is not known yet. Therefore, the Line measurement is used to compute a value, in matrix form, it is represented as:

$$T_1 = T_A T_L T_B \quad (3.46)$$

Solving for T_B, the following product is obtained

$$T_B = T_L^{-1} T_A^{-1} T_1 \tag{3.47}$$

Let T_1 be defined as

$$T_1 = g\begin{bmatrix} d & e \\ f & 1 \end{bmatrix} \tag{3.48}$$

According to the definition if T_A, T_B and T_L (2.20, 2.22 and 2.25), (3.47) is written as

$$T_B = \begin{bmatrix} e^{\gamma L} & 0 \\ 0 & e^{-\gamma L} \end{bmatrix} \frac{1}{\tau_{22}(a-bc)} \begin{bmatrix} 1 & -b \\ -c & a \end{bmatrix} g \begin{bmatrix} d & e \\ f & 1 \end{bmatrix} \tag{3.49}$$

Simplifying the product of the matrices, it is obtained

$$T_B = \frac{g(a-ce)e^{-\gamma L}}{\tau_{22}(a-bc)} \begin{bmatrix} \frac{d-bf}{a-ce} e^{2\gamma L} & \frac{e-b}{a-ce} e^{2\gamma L} \\ \frac{af-cd}{a-ce} & 1 \end{bmatrix} \tag{3.50}$$

The elements of the T_B matrix are found comparing term by term on each side of (3.47). In which α can be found as a function of a/c

$$a\alpha = \frac{d-bf}{1-\frac{c}{a}e} e^{2\gamma L} \tag{3.51}$$

Multiplying (3.51) and (3.45), a is computed as:

$$a_{meas} = \pm \sqrt{\frac{(d-bf)(\Gamma_{M1}-b)\left(1+\frac{\beta}{\alpha}\Gamma_{M2}\right)}{\left(1-\frac{c}{a}e\right)(\varphi+\Gamma_{M2})\left(\frac{c}{a}\Gamma_{M1}+1\right)}} e^{\gamma L} \tag{3.52}$$

From (3.53), a_{meas} is the same a determined as in the calibrations explained in previous chapter.

There is a problem regarding (3.52), which is the sign is not known, this can be solved by using a reflect measurement where we look for an estimated $\hat{a}$

$$\hat{a} = \frac{\Gamma_{M1}-b}{\Gamma_R\left(1-\frac{c}{a}\Gamma_{M1}\right)} \tag{3.53}$$

It is seen that Γ_R is unknown. However, the Γ_R sign is specified as the choice for the reflector such that $\Gamma_R = -1$ for a short circuit or $\Gamma_R = 1$ for an open circuit. There are cases where the reflector element might be offset this is where the reflection coefficient can be expressed as

$$\Gamma_R = \pm|\Gamma_r|e^{-2\gamma L_R} \tag{3.54}$$

where

- L_R is the length of the offset reflect
- γ is the propagation offset constant

As a reflect, the reflection coefficient over the broadband is assumed to be $|\Gamma_r| = 1$. This assumption is substituted in (3.53) to obtain

$$\hat{a} = \frac{\Gamma_{M1} - b}{\left(1 - \frac{c}{a}\Gamma_{M1}\right)} e^{2\gamma L_R} \tag{3.55}$$

As a_{meas} must be equal to $\hat{a}$ equations (3.52) and (3.55) can be equated to obtain the following ratio

$$\frac{\frac{b - \Gamma_{M1}}{\left(\frac{c}{a}\Gamma_{M1} - 1\right)}}{\pm\sqrt{\frac{(d - bf)(b - \Gamma_{M1})\left(1 + \frac{\beta}{\alpha}\Gamma_{M2}\right)}{\left(1 - \frac{c}{a}e\right)(\varphi + \Gamma_{M2})\left(\frac{c}{a}\Gamma_{M1} + 1\right)}}} = e^{\gamma L} e^{-2\gamma L_R} \tag{3.56}$$

Depending on the cases one of the two exponentials will have to be estimated and this is where equation (3.56) is useful.

- $L = 0; L_R \neq 0$
- $L \neq 0; L_R = 0$

Chapter 4

Measurements

Transition embedded DUT measurements were performed, in which the calibration techniques explained in this work were applied in order to compute the actual S parameters. Either in a probe station or in a test fixture, a calibration kit is required. The VNA used for this purpose was the PNA-X and the VNA HP 8510C series.

4.1 Calibration Kits

A calibration kit from J Micro Technology (CM05) was utilized to calibrate on wafer devices (see Fig. 4.1). This calibration kit has many standards needed for different calibration techniques, because of its size, the measurements had to be performed with a Microwave Probe (see Fig. 4.2).

From this work, the standards needed are: Lines, Reflects (Open and Short) and Match. In the CM05 calibration kit shown in Fig. 4.1, these standards are represented as: T (Thru), LT1 (Line 1), LT2 (Line 2), LT3 (Line 3), LT4 (Line 4), S (Short), O (Open), L (Load or Match) and OL (Offset Load or Offset Match), where the reference line is the Thru line. This means that all the other circuits are the same length as the Thru (reference plane) and the standards that have the offset are longer than the Thru length and the Load standards have a 50Ω load matched to the VNA.

On the other hand, a test fixture is used for measuring packaged components. The test fixture is composed of: edge sections where the transition from coaxial

to microstrip is performed and removable mid-sections, where the size of each standard has to be the same size of the mid-section.

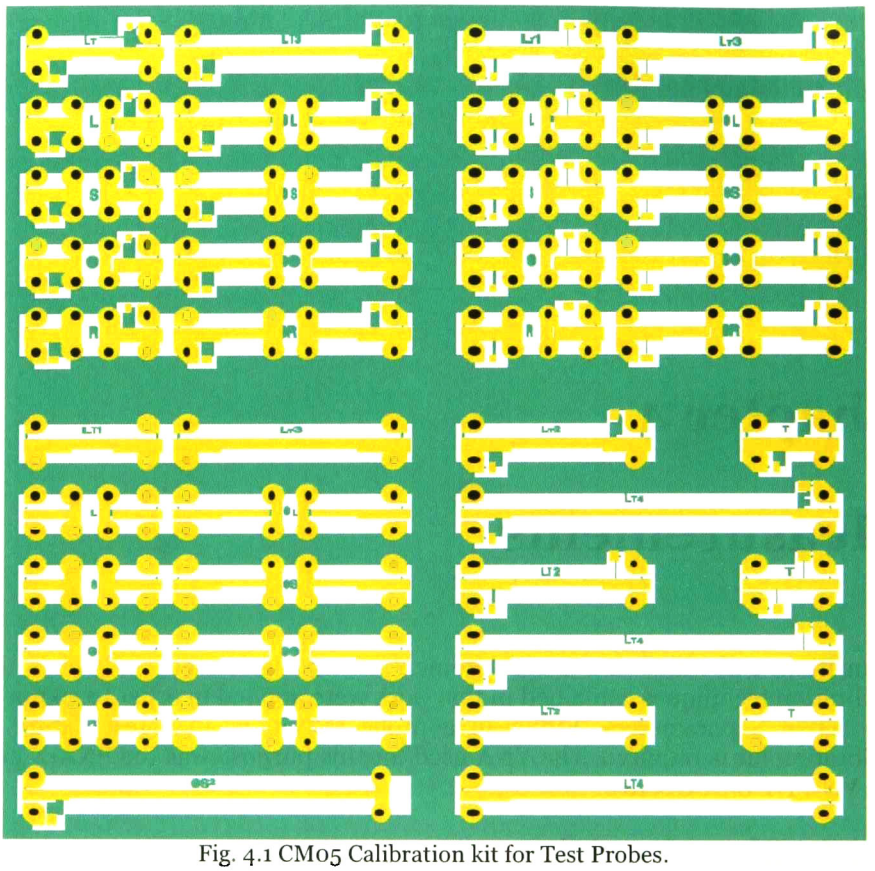

Fig. 4.1 CM05 Calibration kit for Test Probes.

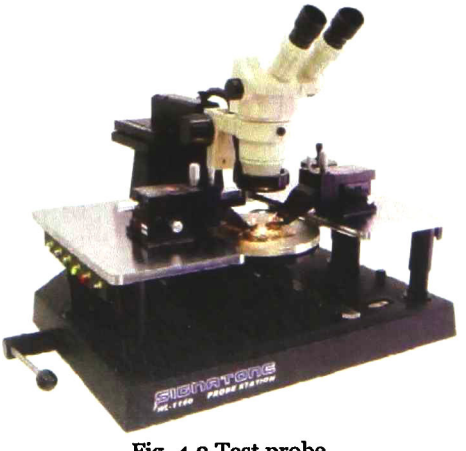

Fig. 4.2 Test probe.

An in-house test fixture was designed and fabricated due to the high cost of a commercial test fixture (see Fig. 4.3).

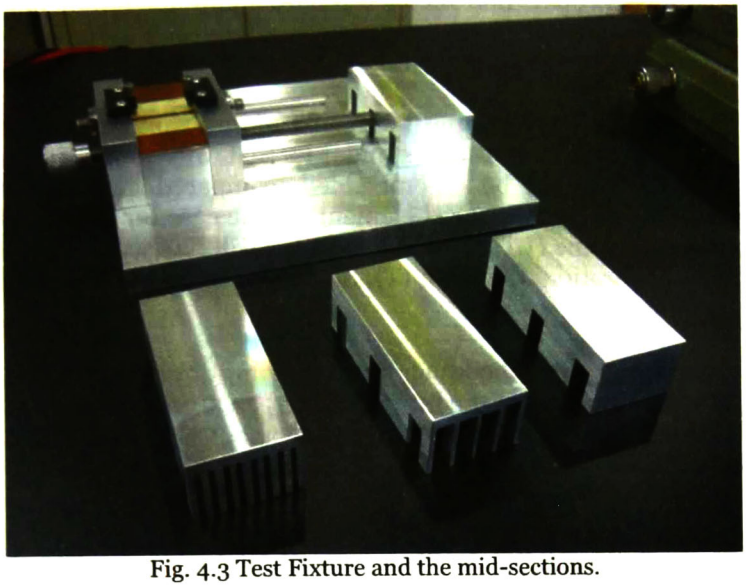

Fig. 4.3 Test Fixture and the mid-sections.

In addition of all the items required for a calibration, an Object Oriented Software in Matlab was developed to obtain and extract the actual S parameters from the measurements done with the VNA.

4.2 TRL and LRRM measurement

Several elements from the CM05 calibration technique were measured in order to validate for the TRL and LRRM algorithms and show the expected behavior commented in this work of some non-reflective lines and reflects.

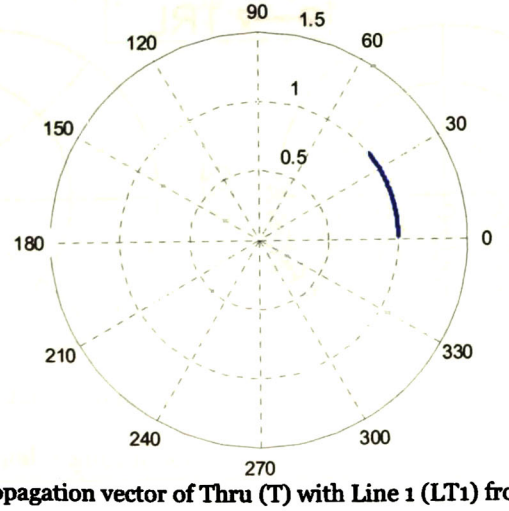

Fig. 4.4 Wave propagation vector of Thru (T) with Line 1 (LT1) from 0.045-20 GHz.

The wave propagation vector of a lossless line measured from the reference plane (Thru) at a frequency range from 0.45-20 GHz is shown in Fig. 4.4. As expected, the wave propagation vector will have a unit magnitude but a change in phase due to the change in the electrical length at each frequency. This plot was performed with the TRL algorithm.

A comparison of the LRRM to the TRL calibration technique is performed to verify them. For this, the same standards that are found in the CM05 calibration technique will be de-embedded, compared and verified to the expected behavior of the measured element. In the case for a TRL calibration, the Thru (T), longer line (LT1) and the short (S) will be used to calibrate while for the LRRM calibration, the Thru (T), Short (S), Open (O) and Load (L) will be used.

Fig. 4.5, shows the de-embedding of LT1 from CM05 calibration kit. As expected, the S parameters of the line is $S_{11} = S_{22} = 0$ and $S_{12} = S_{21} = e^{-jγl}$ for both calibrations, show low losses (Magnitude about 1) and a change in phase due to the change in the electrical length at each frequency. This behavior shows what it is stated in section 3.5.

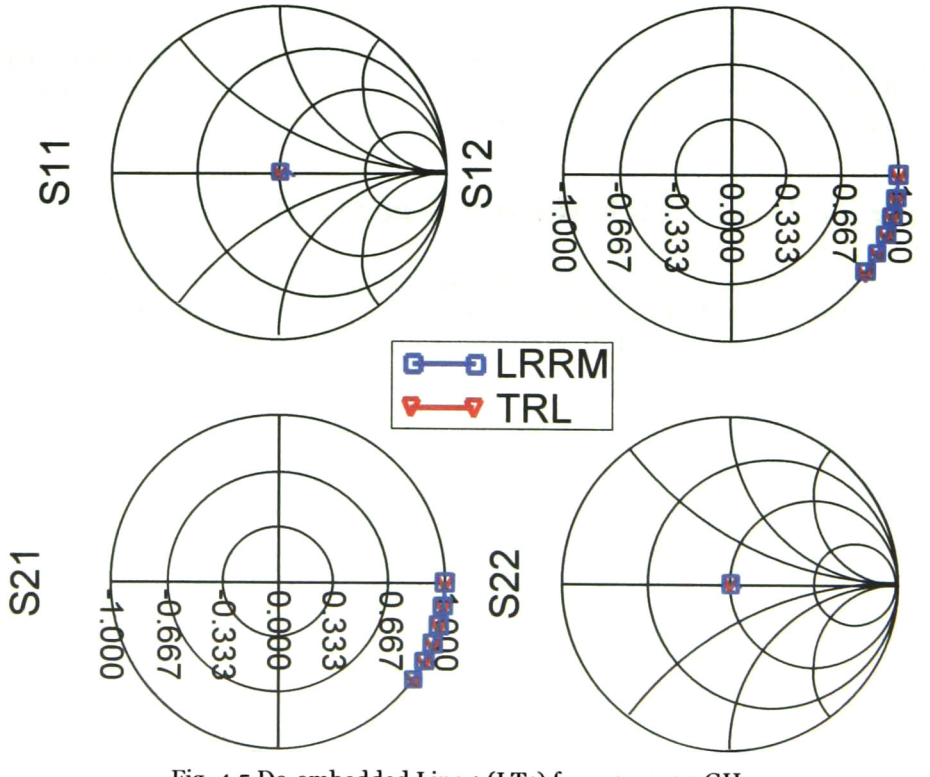

Fig. 4.5 De-embedded Line 1 (LT1) from 0.45-20 GHz.

To show the change in phase three more lines of longer length will be shown (Fig. 4.6 - Fig. 4.8). If a line of longer length than the previous one (LT1) is measured, the $S_{12} = S_{21}$ parameters will show a bigger change in phase.

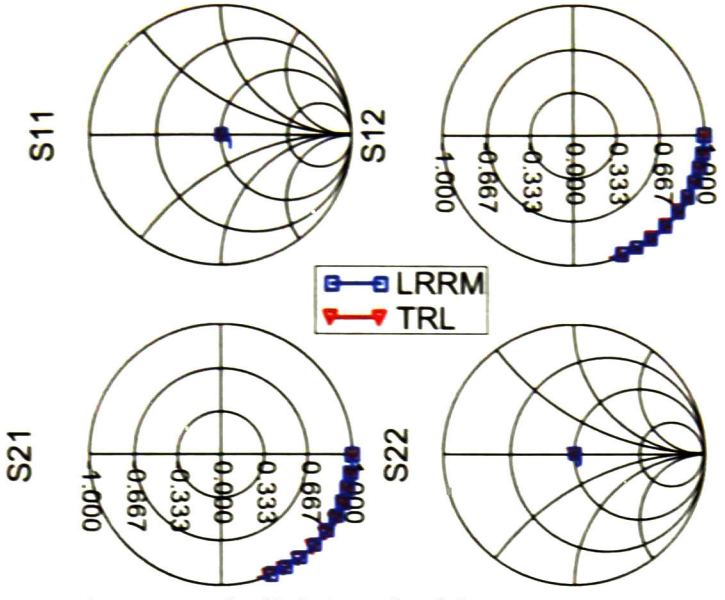

Fig. 4.6 De-embedded Line 2 (LT2) from 0.45-20 GHz.

Line 3 (Fig. 4.7) shows a greater change in phase as expected. The TRL and LRRM calibration technique show no separation between them, showing similar error boxes estimations and therefore no errors in the algorithms.

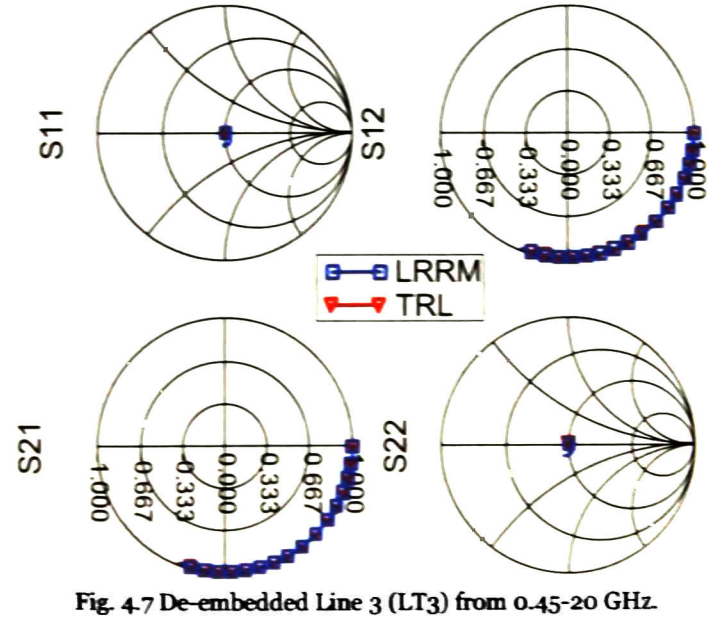

Fig. 4.7 De-embedded Line 3 (LT3) from 0.45-20 GHz.

Fig. 4.8, shows a line that crosses the 180 degrees. If this line (LT4) were used for the TRL calibration, an error in the calibration will exist at points around the 180 degrees crossing of the Line 4 (LT4).

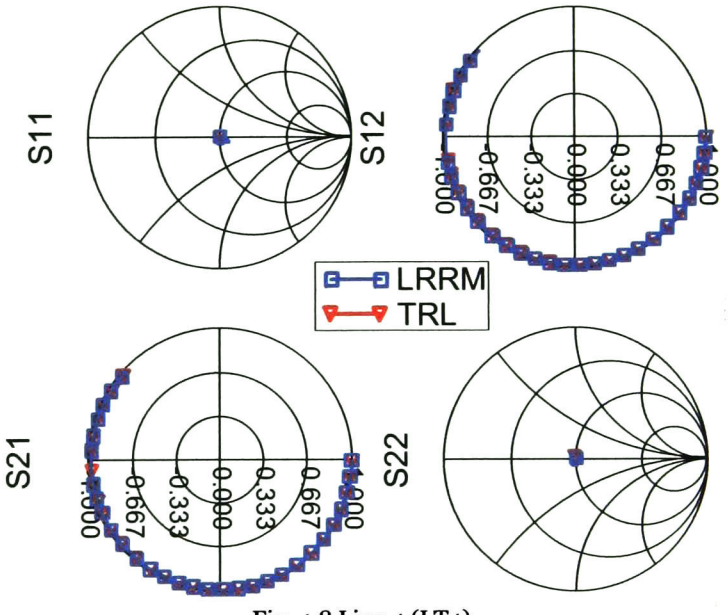

Fig. 4.8 Line 4 (LT4).

A Short (S) without an offset is shown in Fig. 4.9. Although a change in phase is seen the offset is still acceptable, this is due to the probes are difficult if not impossible to position at the reference plane. As a reflect standard the reflection coefficient of a short is $\Gamma = -1$, therefore the S parameters are $S_{11} = S_{22} = -1$ and $S_{12} = S_{21} = 0$.

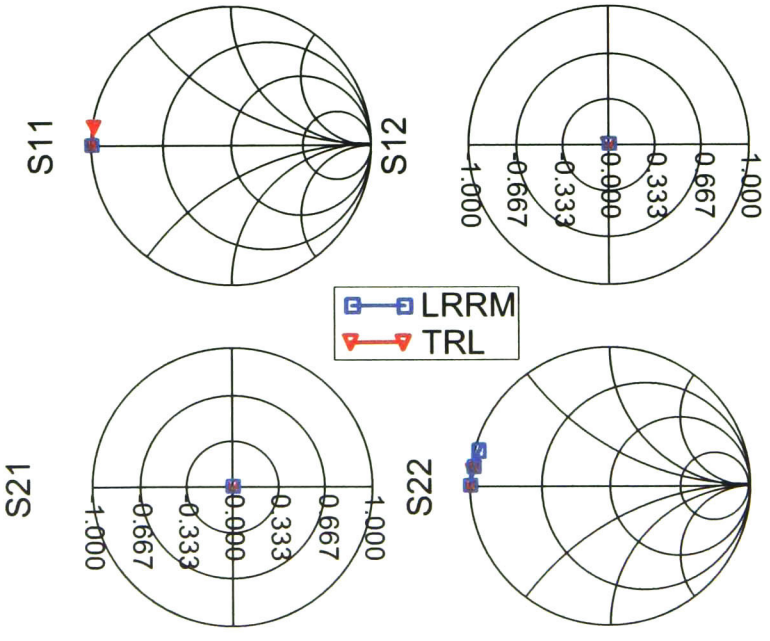

Fig. 4.9 De-embedded Short (S) from 0.45-20 GHz.

The same case applies for the Open (O) standard. There is a change in phase due to the probes that are not positioned at the reference plane and the reflection coefficient of an open standard is $\Gamma = 1$, therefore the S parameters for an open is $S_{11} = S_{22} = 1$ and $S_{12} = S_{21} = 0$.

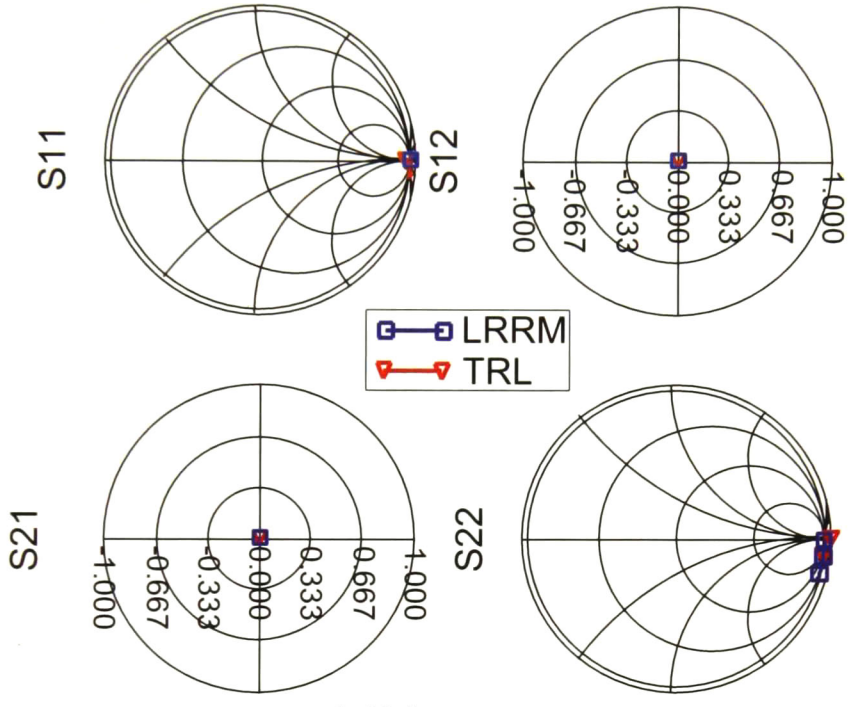

Fig. 4.10 De-embedded Open (O) from 0.45-20 GHz.

4.2.1 TRL error.

TRL calibration technique is said to have an indetermination. This error is present when a 180 degrees difference in electric length of the two lines is found. The product between the lines in the calibration, have an indetermination at the 180 degrees crossing and around.

To show the limitation of the TRL calibration technique, a calibration with a Thru line, a short and a line longer enough that has a 180 degrees of difference in electrical length at a certain frequency was performed with a de-embedding of several lines for the CM05 calibration kit. To show the error physically, a de-embedded line will be enough to show what is stated.

Fig. 4.11 shows a de-embedding of the CM05 line 3 (LT3). At low frequencies, a normal de-embedding is observed as the previous de-embedding, but, as the change in phase increases, the error around the 180 degrees caused by the calibration becomes evident. As can be seen the error is present around 90 degrees.

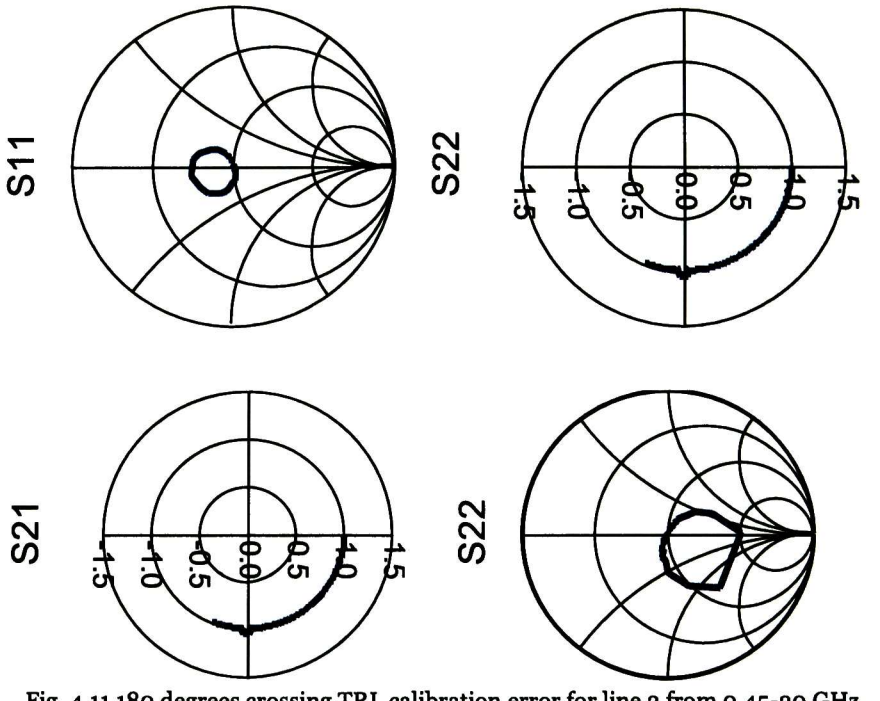

Fig. 4.11 180 degrees crossing TRL calibration error for line 3 from 0.45-20 GHz.

4.3 Transistor measurement

Both calibrations, TRL and LRRM were performed on a test fixture to compare the S parameters of a transistor obtained at a certain bias point. Two tier calibration is performed, this means, the reference plane is set to the bound of the VNA cables (Fig. 4.12). When either the TRL or LRRM calibration is performed the reference plane is now set to the middle of the Thru (Fig. 4.13).

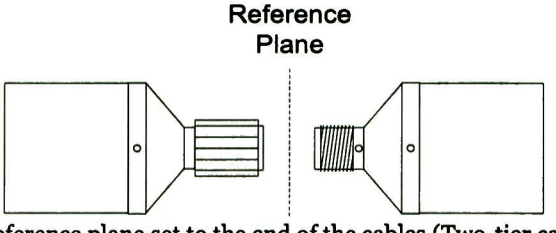

Fig. 4.12 Reference plane set to the end of the cables (Two-tier calibration).

The test fixture showed several limitations, the majority were mainly mechanical. The measurements performed showed a difference in port 1 and port 2 where the root cause was found to be the unevenness of the pressure at each port. As the edge sections act as a press, one edge section is fixed while the other edge section is movable, causing a slight movement to all sides, in consequence, a repetitive and symmetric measurement is difficult to achieve.

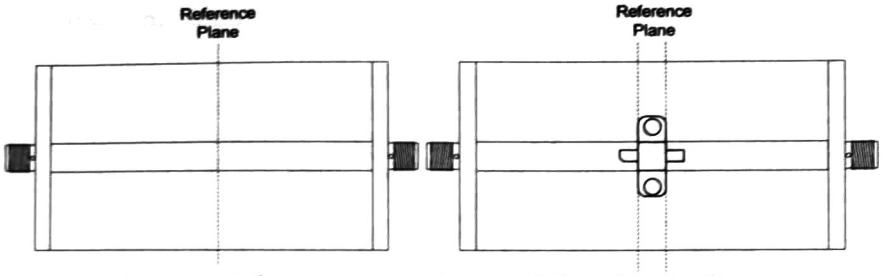

Fig. 4.13 Reference plane set to the middle of the Thru line.

Two test fixtures with different characteristics were designed and tested in order to eliminate variables and to find the root causes of the errors. One test fixture was fabricated with molten aluminum, while the other was made of commercial aluminum. The results were better for the molten aluminum than for the commercial aluminum test fixture.

In order for the measurements to work, the pin of the connector has to be pressed down, however, this generates a bending in the pin if high pressure is applied to the edge-section. The bending in the pin distorts the measurements due to the uneven contact of the pin to the circuit. Moderate pressure showed an improvement in the measurements, but still, the pressure in the fixed edge-section is not the same as in the movable edge-section because of the free movement.

It is also seen that the longer the distance between the reflects the less coupling between them, resulting in a better calibration. On the other hand, the quality of the elements defines the range for the calibration. The vias hole in the reflects works as expected at low frequencies, but as the frequency is increased the return losses at both ports are lowered. The same case applies for the match, where the vias hole and the welling of the load limit the measurement range.

A solution for the test fixture is to allow a vertical and horizontal movement for both edge sections, this will help in adjusting the pressure at each port. Another important improvement due to the vertical and horizontal movement will be the independency of the substrate height and thickness and avoid the damage on the edges of the circuits caused by the connectors when they are moved closer to contact the circuit.

To analyze the strengths of the calibration techniques, two-tier calibration data is shown in Fig. 4.14 for a packaged GaN transistor, model CGH40010F ($V_{gs} = -3\,V$ and $V_{ds} = 28\,V$ from 0.5-6 GHz) is shown. This shows the measurement of the transistor embedded between two transmission lines with the corresponding transition from coaxial to microstrip,

Fig. 4.14 and Fig. 4.15 shows how the de-embedding process works for the transistor where the two-tier calibration measurement shows a big change in the phase, due to the transmission lines embedded within the S parameters of the transistor. This change and the transition errors are eliminated by the TRL and LRRM calibration and further de-embedding because the reference plane

has been set to the middle of the Thru which is equal to the lines where the transistor is embedded.

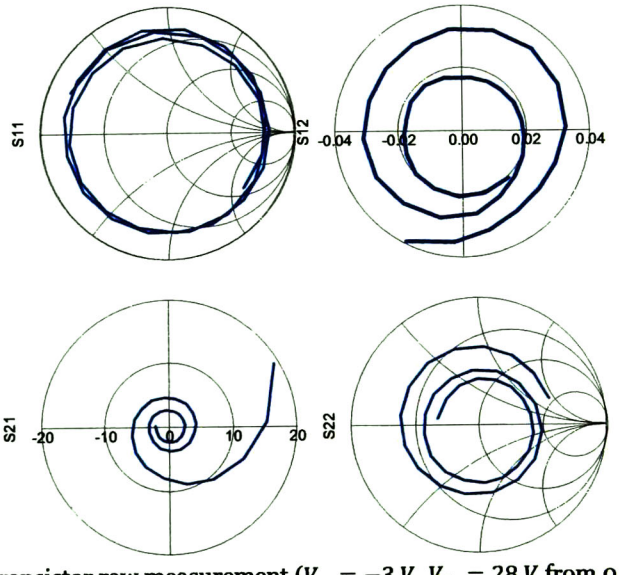

Fig. 4.14 Transistor raw measurement ($V_{gs} = -3\,V$, $V_{ds} = 28\,V$ from 0.5-20 GHz).

In Fig. 4.15, the triangles curves show the transistor S parameters measured and corrected with a TRL calibration; the squares curves is the corresponding parameters measured and corrected with a LRRM calibration.

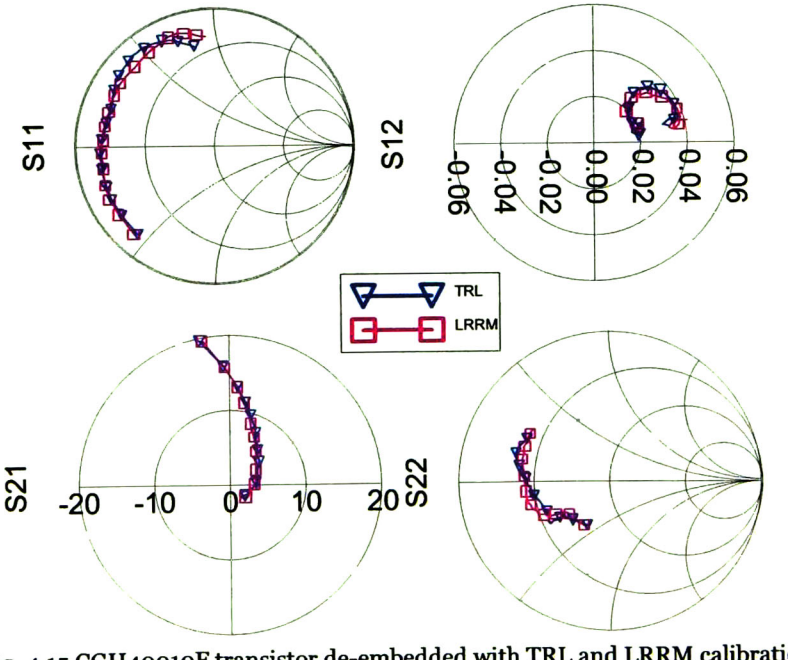

Fig. 4.15 CGH40010F transistor de-embedded with TRL and LRRM calibration technique ($V_{gs} = -3\,V$ and $V_{ds} = 28\,V$).

Both calibrations appear to be consistent with each other with a slight difference at S_{11} and S_{22} parameters. The difference in S_{11} and S_{22} is caused by the difference in the measurement of the Reflects (Short and Open) and Matching (Load) standards. Even though the Short and Open circuits behaves similarly in magnitude, there were differences in the measurement around 3 GHz, causing the slight deviation in the error box estimation.

Chapter 5

Conclusions and future work

The calibration techniques always have to be performed in order to obtain actual measurement of a DUT. Its selection will depend on the needs of the measurement, that is, cost, implementation and the accuracy.

The TRL and LRRM standards do not need to be completely known as compared to the SOLT standards, this is why SOLT technique algorithm is more complicated than any other calibration technique for packaged or on wafer networks.

With the TRL and LRRM calibration technique, the reference plane is set at the middle of the reference transmission (Thru) line no matter which technology is applied. In addition, when working with non-coaxial technology, that is, for in fixture and coplanar technology, the SOLT present a limitation because its fabrication is very difficult. In consequence, the cost of producing the TRL and LRRM standards are much lower.

TRL calibration technique has a limitation, when the difference in electrical length of the reference line (Thru) and the Line is 180 degrees, the computation presents indeterminations, yielding misleading results.

All the calibration techniques present limitations depending on the quality of the components (i.e.: substrate, vias hole, loads and connectors). In this case LRRM calibration technique was mainly limited by the resistor used, even though the data sheet assured the resistor worked at a wide frequency range, the process of making the vias and the welling utilized in this work, reduced its quality.

It was seen that the test fixture material was not as important as any other feature like the substrate, the vias hole, the connectors and how the connectors make contact with the substrate. This was proved on the two test fixtures that were fabricated that showed similar results.

In addition, it was seen that even if the circuit was not the same size as the mid-section of the test fixture but approximately the size of the mid-section, specifically smaller, good results were still obtained. In contrast, with circuits slightly larger than the mid-section of the test fixture, repeatability was hard to find and a stressing of the substrate was found because the horizontal pressure of the edges curved the circuits avoiding full contact of the connector pins.

Better results in the reflect measurements were observed, as they were moved away from each other. This caused less coupling effect from port 1 to port 2 and vice versa, but still a limitation existed because of the vias hole in the circuits. A more professional fabrication of the circuits would have been better to eliminate the circuit variable from all the mechanical limitations from the test fixture.

Improving the test fixture will require high cost and work to find the better design. A mechanical engineer could have helped to solve all the mechanical requirements, such as, horizontal and vertical movement, taking care of the pressure and a complete contact of the pin of the connector to the transmission lines of the circuits that will be placed in the mid sections.

Work with different substrates and different heights and thickness will help to determine the features that a substrate must have in order to have a better performance for the calibration. As it was explained prior, thinner and high dielectric constant substrate, will provide less field leakage than a wider and low dielectric constant substrate.

There are many manufacturers that can fabricate the standards and circuits needed for calibration and measurement of a packaged transistor or RF circuit. The problem is the cost, but the precision and quality of the vias hole, and the traces will improve considerably the frequency range of the test fixture.

In this work an object oriented software was developed in Matlab and its proper documentation which performs the basic proceedures: VNA communication, TRL, LRRM, de-embedding (Straight-forward and Classic method), parameter conversion (T to S parameter and viceversa), plotting and saves the data into a touchstone file.

The classes programmed so far, serve as the core for a bigger software development with easy maintenance, debug and adding of modules. This is why this software was developed using object oriented programming (OOP), because it provides better administration in all the senses compared to a structured programming.

Future calibrations will have to be added, different VNAs will be connected and a friendly Graphical User Interface (GUI) will have to be implemented and modified continuously, hence, modification of the software will be imminent as

to the daily maintenance. An intuitive and friendly GUI development of the software will be a high priority for new users.

If new calibrations are to be proved, the necessary programming will have to be done and added to the software with the necessary modifications of the other classes that interact with it.

The software probably will work in other place and with other VNAs, so the corresponding modules for the other VNAs will have to be added. An advantage of the software is that the VNA communication is made by an interface, this means that, the code of the implemented class that communicates with a specific VNA will have to comply with the protocol stated by the interface, this was performed in order to have the minimum modification as possible for third party classes of the program.

Appendix A

Linear Algebra

If T and T_Ψ are similar matrices then the determinants are similar too

$$\det(T) = \det(T_\Psi) \tag{A.1}$$

$$A = T_v B T_v^{-1} \tag{A.2}$$

$$\det(A) = \det(T_v)\det(B)\det(T_v^{-1}) \tag{A.3}$$

Hence,

$$\det(A) = \det(B) \tag{A.4}$$

Two similar matrices have their own characteristic polynomial and hence, their own characteristic values

$$\det(\lambda I - T) = \det(\lambda I - T_\Psi) \tag{A.5}$$

Two similar matrices have the same trace (abbreviated as tr)

$$tr(T) = tr(T_\Psi) = t_{11} + t_{22} = \Psi_{11} + \Psi_{22} \tag{A.6}$$

Appendix B

Codes

In this appendix the Matlab codes for the calibration techniques developed in this work are shown to help the reader understand and demonstrate that the calibrations works just by copying the code and pasting it into a m Matlab file as a function. The function must receive the S-parameters depending on the standards required and the error boxes will be returned in order to use them later for the de-embedding process either straightforward or the classic.

B.1 TRL Matlab function.

```
function [Ta, Tb, rho22r22, psi]=TRL(Thru, Line, Reflect, Gamma)
% TRL calibration technique
% It needs 3 caalibration standars
% -Two non-reflective lines Lref (shortest considered Thru) & L2
% -High reflection coefficient element (reflect) (short circuit or open
% circuit)
%
% Thru (Thru measured S-parameters)
% Line (Line measured S-parameters)
% Reflect (Reflect measured S-parameters)
% Gamma (Reflection coefficient 1 for Open -1 for Short)
%

% Convert Thru and Line S-parameters to T-parameters for cascading
T1=StoTparams(Thru);
T2=StoTparams(Line);

[row,col,deep]=size(Thru);

% Variable initialization
T=zeros(row,col);
Ta=zeros(row,col,deep);
Tb=zeros(row,col,deep);
```

```
rho22r22=zeros(deep,1);
psi=zeros(deep,1);

%sweep all matrices in order to calibrate
for i=1:deep
  T(:,:)=T2(:,:,i)/T1(:,:,i);

  %% Error box A computation
  % b computation
  r=roots([T(2,1),(T(2,2)-T(1,1)),-T(1,2)]);
  % the smallest absolute number must be b
  % as the condition must be satisfied |b|<|a/c|
  if (abs(r(1,1))) < (abs(r(2,1)))
    b=r(1,1);
    a_c=r(2,1);
  elseif (abs(r(1,1))) > (abs(r(2,1)))
    a_c=r(1,1);
    b=r(2,1);
  else
    error('Equal roots')
  end

  %% Propagation wave vector
  psi(i)=(T(2,2)+b*T(2,1)-(b/(a_c))*T(1,1)-(1/(a_c)*T(1,2)))/(1-b/(a_c));
  %psi(i)=(1-b/(a_c))/(T(1,1)+1/(a_c)*T(1,2)-b*T(2,1)-(b/(a_c)*T(1,2)));

  %% Partial Error Box B computation
  % Put the measured Thru as the form of
  %     +-  -+
  %     | d  e |
  %   T=g|     |
  %     | f  1 |
  %     +-  -+
  g=T1(2,2,i);
  T1(:,:,i)=T1(:,:,i)/g;
  d=T1(1,1,i);
  e=T1(1,2,i);
  f=T1(2,1,i);

  beta_alpha=(e-b)/(d-b*f);
  phi=(a_c*f-d)/(a_c-e);

  %% a error coefficient computation
  n1=d-b*f;
  n2=b-Reflect(1,1,i);
  n3=1+beta_alpha*Reflect(2,2,i);
  d1=1-e/a_c;
  d2=phi+Reflect(2,2,i);
  d3=Reflect(1,1,i)/a_c-1;

  % The exponential term is off the equation because of reference plane
  a_val=sqrt((n1*n2*n3)/(d1*d2*d3));%*exp(gamma*Lref);

  a_est=(b-Reflect(1,1,i))/(Gamma*(Reflect(1,1,i)/a_c-1));

  % error function
  pos_a=abs(a_val-a_est);
  neg_a=abs(-a_val-a_est);

  if pos_a<neg_a
    a=a_val;
  else
    a=-a_val;
```

```
    end

    c=a/a_c;

    Ta(:,:,i)=[a b;c 1];

    %% B error box computation
    % as a is needed we can compute it in the end
    alpha=(d-b*f)/(a-c*e);
    beta=(e-b)/(a-c*e);

    Tb(:,:,i)=[alpha beta; phi 1];
    rho22r22(i)=g*(a_c-e)/(a_c-b);

end
```

B.2 LRRM Matlab function

```
function [Ta]=LOSM(Line, Open, Short, Match)
%
%  function [Ta]=LOSM(Line, Open, Short, Match)
%
% This function obtain the necessary standards to estimate
% the error box for a VNA
%
% Input
% Line: used to compute the Thru Standard in S-params
% Open: used to compute Reflect Standard with Gamma=1
% Short: used to compute Reflect Standard with Gamma=-1
% Match: used to compute a Gamma=0
%
% Output
% Ta: error adapter for the VNA
%

%% Variable initialization
[row, col, deep]=size(Line);
Ta=zeros(row,col,deep);

% reflection coefficient Open
w1=zeros(deep,1);
w2=zeros(deep,1);

% reflection coefficient Short
u1=zeros(deep,1);
u2=zeros(deep,1);

b=zeros(deep,1);
c_a=zeros(deep,1);
%phi=zeros(deep,1);

d=zeros(deep,1);
e=zeros(deep,1);
f=zeros(deep,1);

%% Variable setting
w1(:,1)=Open(1,1,:);
w2(:,1)=Open(2,2,:);
u1(:,1)=Short(1,1,:);
u2(:,1)=Short(2,2,:);

clear Open Short
```

```
% Here the reflection coefficients are equalized by its Gamma real
% and develop the products so to obtain a polynomial that will need to be
% solved by the Thru connection and the Match

%% b and phi values are obtained directly from the match
b(:,1)=Match(1,1,:);
%phi(:,1)=Match(2,2,:);

%% Thru measured
%      +-  -+
%      | d  e |
%  M_T=g|     |
%      | f  1 |
%      +-  -+
M_T=StoTparams(Line);
d(:,1)=M_T(1,1,:)./M_T(2,2,:);
e(:,1)=M_T(1,2,:)./M_T(2,2,:);
f(:,1)=M_T(2,1,:)./M_T(2,2,:);

% we find alpha_beta function depending on b to eliminate unknown values
alpha_beta=(e-b)./(d-b.*f);

% x & y are defined so to reduce the equation's length
x=(b-w1).*(1+alpha_beta.*w2);
y=(b-u1).*(1+alpha_beta.*u2);

% ks' are defined to reduce equation's length
k1=x./y.*u1.*u2-w1.*w2;
k2=x./y.*u1-w1;
k3=x./y-1;
k4=x./y.*u2-w2;

% Set variable poly to make readable the code
poly=[k1.*e+d.*k2, -(k1+f.*k2+d.*k3+e.*k4), f.*k3+k4];

% polynomial root solving
for i=1:deep
  % normally I will have two values as we have only 2nd order polynomials
  c_aRoots=roots(poly(i,:));

  %keep the c/a min value as the other root is the same value as b
  if ( abs(c_aRoots(1)) < abs(c_aRoots(2)) )
    % take a_cRoots(1)
    c_a(i)=c_aRoots(1);
  else
    % take a_cRoots(2)
    c_a(i)=c_aRoots(2);
  end
end

% I can take either the open or short but for now I take the Open so I have
%  a=(b-w1)/(c/a*w1-1)
a=(b-w1)./(c_a.*w1-1);
c=c_a.*a;

Ta(1,1,:)=a;
Ta(1,2,:)=b;
Ta(2,1,:)=c;
Ta(2,2,:)=ones(deep,1);

end
```

References

[1] J. A. Saldívar Morales "Two different philosophies of the LRL multilines calibration technique to correct the systematic errors of a Vectorial Network Analyzer". 2005.

[2] G. F. Engen & C. A. Hoer "Thru-Reflec-Line: An improved technique for calibrating the dual Six-Port Automatic Network Analyzer" IEEE Trans. Microwave Theory and Tech, 1979. 27 (12): 987-993p.

[3] D. M. Pozar "Microwave Engineering", 3rd Edition, 2005, Wiley, Massachusetts, U.S.A.

[4] G. Gonzalez "Microwave transistor amplifiers: analysis and design", 2nd Edition, 1996, Prentice Hall, U.S.A.

[5] Agilent AN 1287-1, "Understanding the Fundamental Principles of Vector Network Analysis" Application Note, 1997.

[6] Z. Skvor and K. Hoffmann. "A Novel Vector Network Analyzer", IEEE Trans. Microwave Theory Tech. vol. 46, No. 12, Dec. 1998. pp. 2520-2523

[7] Scott A. Wartenberg "RF measurements of die and packages", Artech House microwave library, 2002.

[8] R. Ludwig, Pavel Bretchko, "RF Circuit Design, Theory and Applications" Prentice Hall, 2002, New Jersey, pp. 192-198.

[9] J. E. Zuñiga Juares "LRL, LRM and TRRM Calibration techniques for systematic error correction of a Vector Network Analyzer and their impact in the high frequency transitors characterization", Mex. 2011.

[10] E. Anderson "Robust Triangular Solves for Use in Condition Estimation" Eagan, MN, USA, 1991.

[11] J. A. Reynoso-Hernandez, "Reliable Method for Computing the phase Shift of Multiline LRL Calibration Technique", IEEE Microwave and Wireless Components Letters, vol. 12, pp 395-397, October 2002.

[12] J. A. Reynoso-Hernandez, E. Inzunza "A straightforward de-embedding method for devices embedded in test fixtures", 57th ARTFG Conference Digest, vol. 39, pp. 1-5, May 2001.

[13] R. A. Hackborn "An automatic network analyzer system", Microwave J., pp. 45-52, 1968.

[14] D. Rytting, "Network analyzer error models and calibration methods" Hewlett-Packard Company, 1998.

[15] J. A. Reynoso-Hernández, "Unified method for determining the complex propagation constant of reflecting and non-reflecting transmission lines" IEEE Microwave and Guided Wave Letters, vol. 13, pp. 351-353, August 2003.

[16] J. A. Reynoso-Hernández, "On wafer calibration technique using a non-reflectin lossy line of arbitrary length" 63rd Automatic RF Techniques Group Conference Digest, pp. 205-210, Fort Worth, TX, June 2004.

[17] R. Mongia, I. Bahl, P. Bhartia, "RF and microwave coupled-line circuits" Arthec House microwave library. MA, 1999.

[18] K. Kurokawa, "Power Waves and the Scattering Matrix", IEEE Microwave Theory Techniques, vol. 13, pp. 194-202, New Jersey, March 1965.

[19] H. A. Wheeler, "Transmission-line properties of parallel wide strips by a conformal-mapping approximation", IEEE Trans. Microwave Theory Tech., vol. MTT-12, pp. 280-289, May 1964.

[20] R. B. Marks, "A multiline method of network analyzer calibration", Microwave Theory and Techniques, IEEE Transactions, vol. 39, pp. 1205-1215, Boulder, CO, USA, Jul. 1991.

[21] N. R. Franzen and R. A. Speciale, "A new procedure for system calibration and error removal in automated S-parameter measurements," Prox. 5th European Microwave Conf. (Hamburg, Germany, Sept. 1-4, 1975), pp. 69-73.

[22] R. A. Speciale, "A generalization of the TSD network-analyzer calibration procedure, covering n-port scattering parameter measurements, affected by leakage errors," IEEE Trans. Microwave Theory Tech., vol. MTT-25, pp. 1100-1115, Dec. 1977.

[23] H. J. Eul and B. Schiek, "Thru-match-reflect: One result of a rigorous theory for de-embedding and network analyzer calibration," Proc. 18th European Microwave Conference, pp. 909-914, Sept. 1988.

[24] J. T. Barr and M. J. Pervere, "A generalized vector network analyzer calibration technique," 34th ARFTG Conf. Dig. (Ft. Lauderdale, FL), Dec. 1989.

[25] I. G. Stanley, "Elementary linear algebra" 5th ed. Brooks/Cole Pub Co. January 2, 1994.

[26] J. A. Jargon, R. B. Marks, D. F. Williams, "Coaxial Line-Reflect-Mach Calibration" Asia-Pacific Microwave Conference Proceedings, pp. 86-89, Taejon, Korea, October, 1995.

[27] Hewlett Packard, "In-fixture measurements using Vector Network Analyzer." Application Note 1287-9, Hewlett Packard

[28] D. Metzeger, "Improving TRL Calibrations of Vector Network Analyzers", Microwave Journal, vol. 38, pp. 56-68, May 1995.

[29] Agilent Technologies, "Specifying Calibration Standards for the Agilent 8510 Network Analyzer" Product Note 8510-5B.

[30] R. R. Pantoja, M. J. Howes, J. R. Richardson, R. D. Pollard, "Improve Calibration and Measurement of the Scattering Parameters of Microwave Integrated Circuits", IEEE Trans. Microwave Theory Tech. vol. 37, No. 11, pp. 1675-1679, November 1989.

[31] F. Purroy, L. Pradell, " New theoretical Analysis of the LRRM Calibration Technique for Vector Network Analyzers", IEEE Transactions on Instrumentation and Measurement, vol. 50, No. 5, October 2001.

[32] R. F. Bauer, P. Penfirld, "De-embedding and unterminating". IEEE Transactions on Microwave Theory Tech, 22, pp. 282-288.

CENTRO DE INVESTIGACIÓN Y DE ESTUDIOS AVANZADOS DEL I.P.N.
UNIDAD GUADALAJARA

El Jurado designado por la Unidad Guadalajara del Centro de Investigación y de Estudios Avanzados del Instituto Politécnico Nacional aprobó la tesis

Diseño e Implementación de la técnica de calibración LRRM
Design and Implementation of the LRRM Calibration Technique

del (la) C.

Diego OROZCO NAVARRO

el día 01 de Febrero de 2012.

Dr. Pablo Moreno Villalobos
Investigador CINVESTAV 3C
CINVESTAV Unidad Guadalajara

Dr. Federico Sandoval Ibarra
Investigador CINVESTAV 3B
CINVESTAV Unidad Guadalajara

Dr. José Raúl Loo Yau
Investigador CINVESTAV 2C
CINVESTAV Unidad Guadalajara

Dra. Susana Ortega Cisneros
Investigador CINVESTAV 2A
CINVESTAV Unidad Guadalajara

Dr. J. Apolinar Reynoso Hernández
Investigador Titutlar C
CICESE